Environmental Fluid Dynamics: Lecture 2

Dr. Jeremy A. Gibbs

Department of Mechanical Engineering
University of Utah

Spring 2017

Overview

1. Near-Surface Radiation Balance

2. Near-Surface Thermal Radiation

Near-Surface Radiation Balance

Energy Balance over Salt Flats

Utah's West Desert

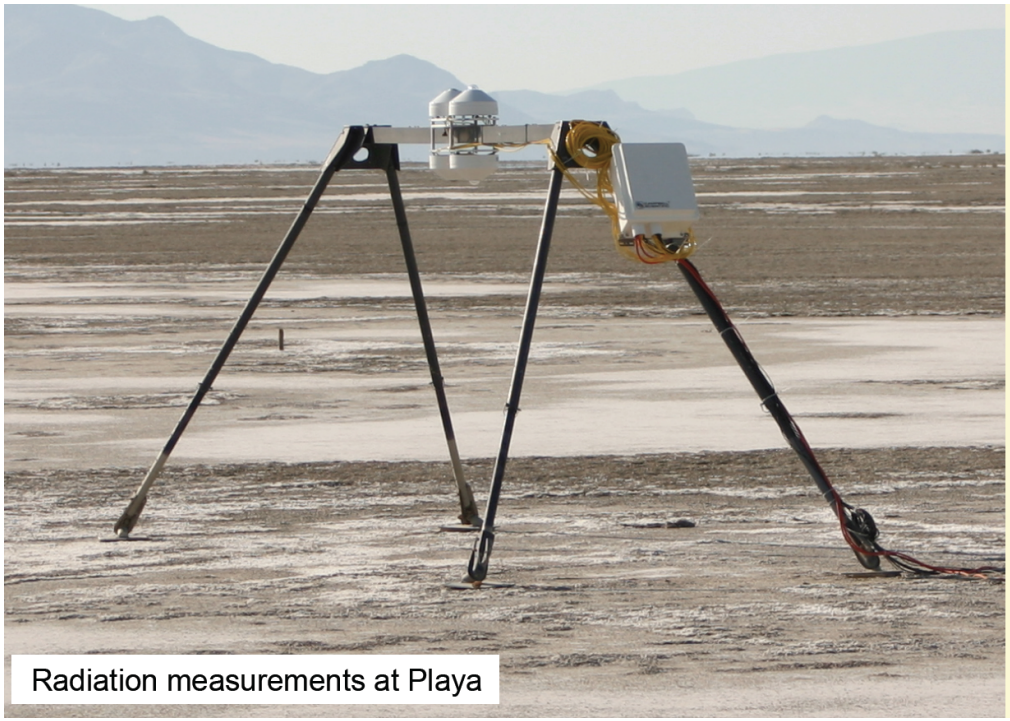

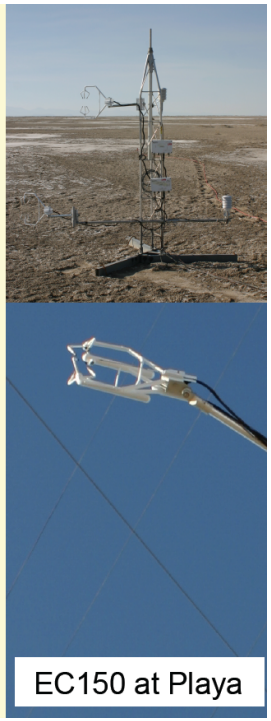

Hoch et al. (2014)

Energy Balance over Salt Flats: Total Balance

$$R_N = H + LE + G + \eta$$

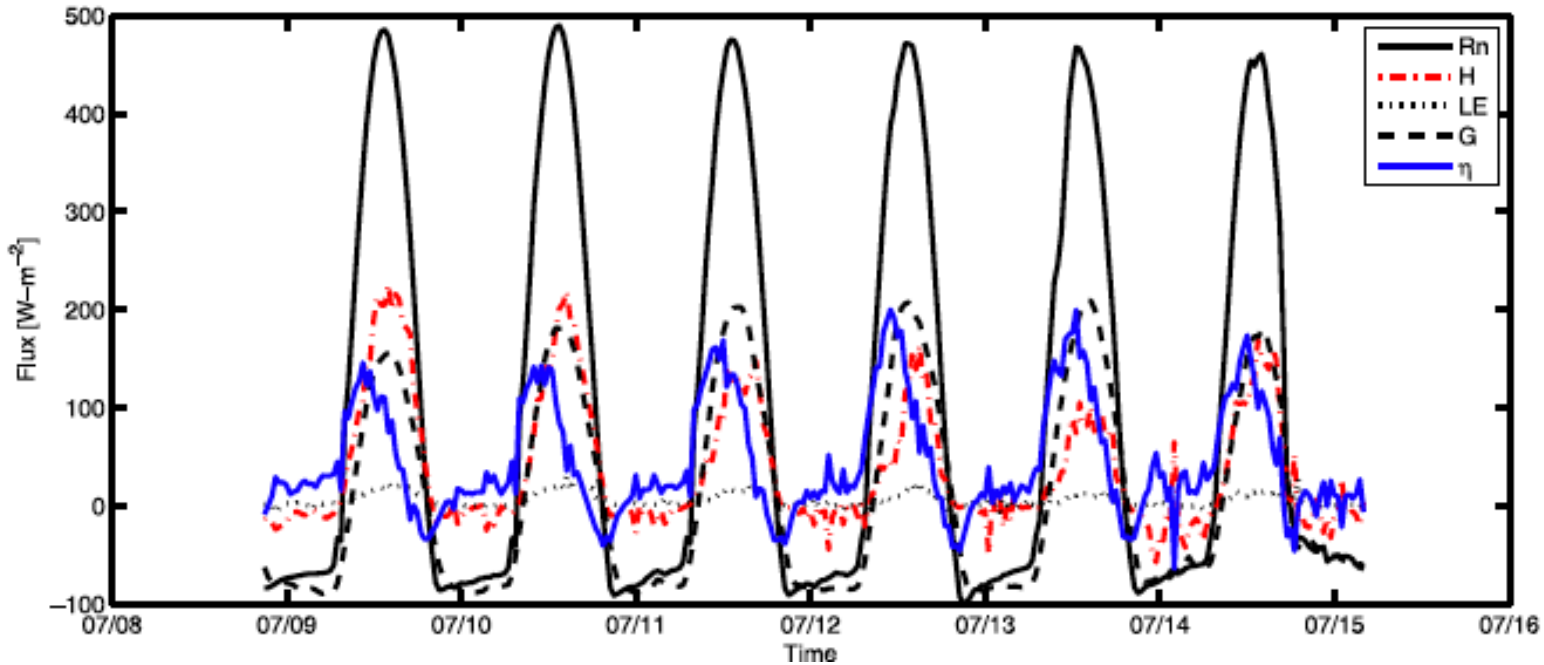

Higgins et al. (2012)

Energy Balance over Salt Flats: Residual Components

$$R_N = H + LE + G + \boxed{\eta}$$

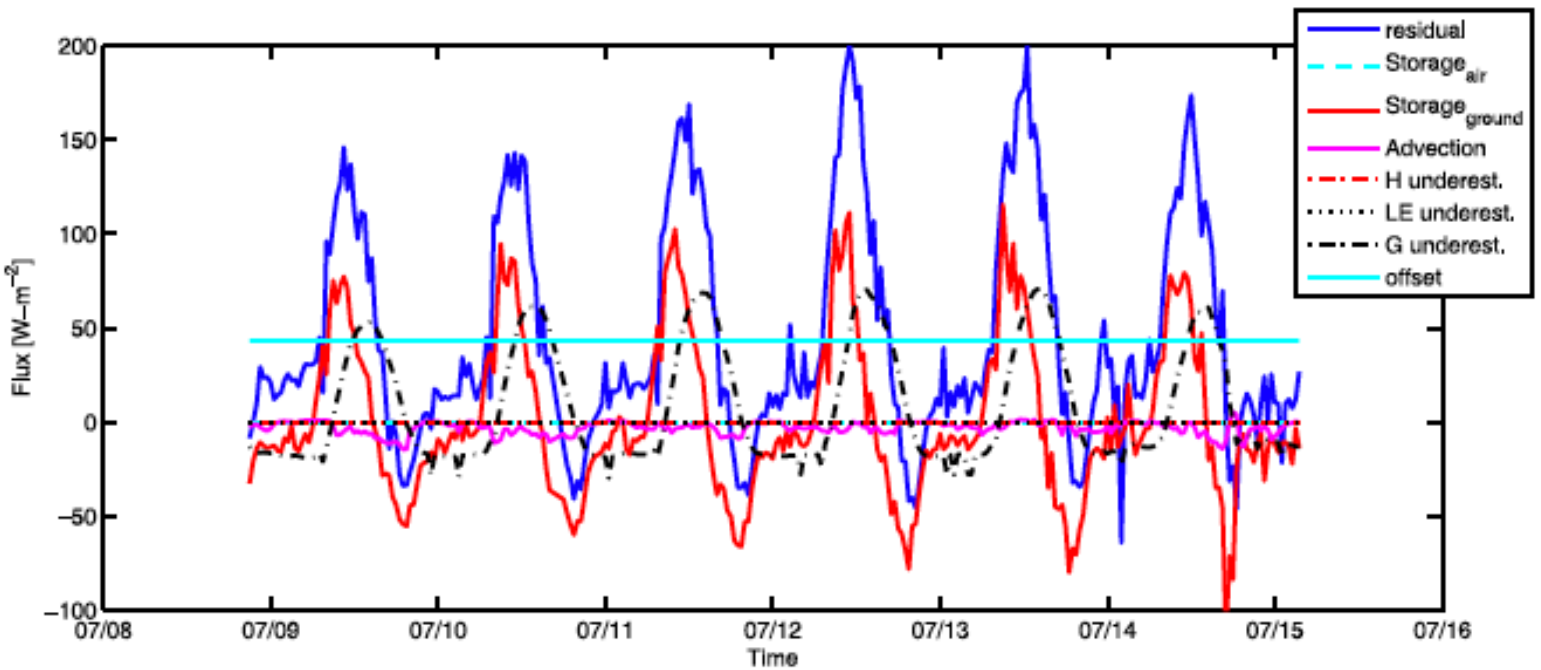

Higgins et al. (2012)

$$\eta(t) = S(t) + A(t) + W(t) + O_T(t)$$

Energy Balance over Salt Flats: Residual Components

$$R_N = H + LE + G + \boxed{\eta}$$

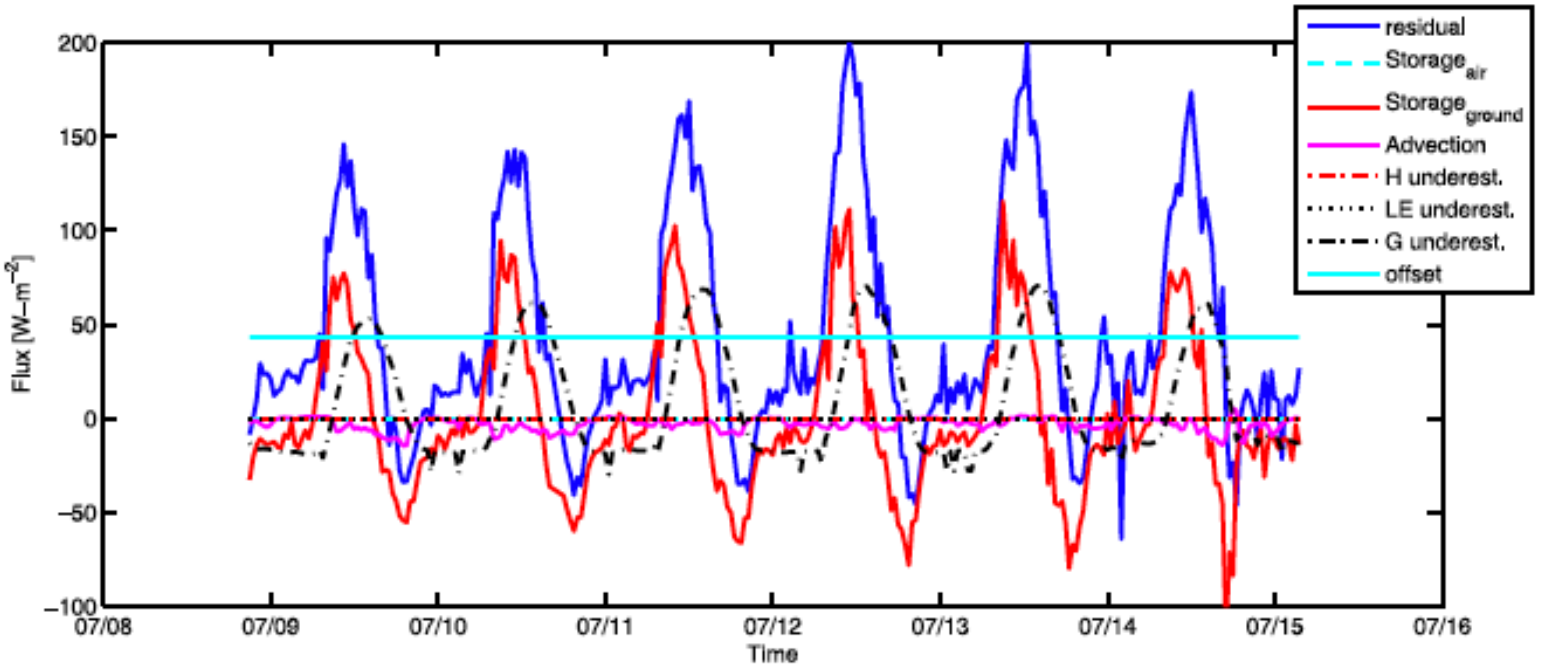

Higgins et al. (2012)

- 59% energy storage in the soil layer
- 30% underestimates of the soil heat flux
- 1% percent advection (not statistically significant)

Near-Surface Thermal Radiation

Near-Surface Thermal Radiation

Radiation

Transfer of energy through rapid oscillation of electromagnetic fields

$$R_N = H + H_L + H_G + \Delta H_S$$

$$R_N = R_S(\downarrow) + R_S(\uparrow) + R_L(\downarrow) + R_L(\uparrow)$$

See Chapter 3 in Arya

Electromagnetic Spectrum

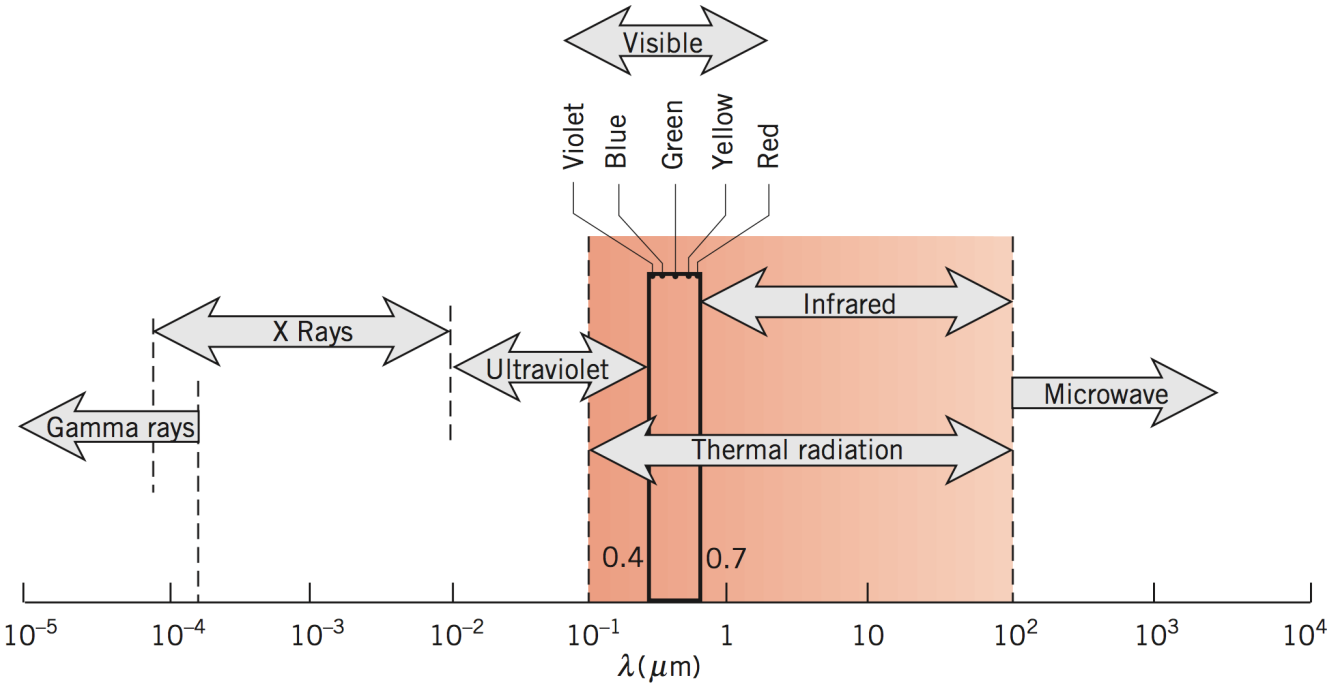

figBergman et al. (2011)

Range of interest for atmospheric radiative transfer
solar $\sim$0.1-4 μm (short wave), terrestrial $\sim$3-100 μm (long wave)

Absorption of Radiation

- Orbital changes in electrons
- Molecular vibration changes
- Molecular rotation changes

Radiation Characteristics

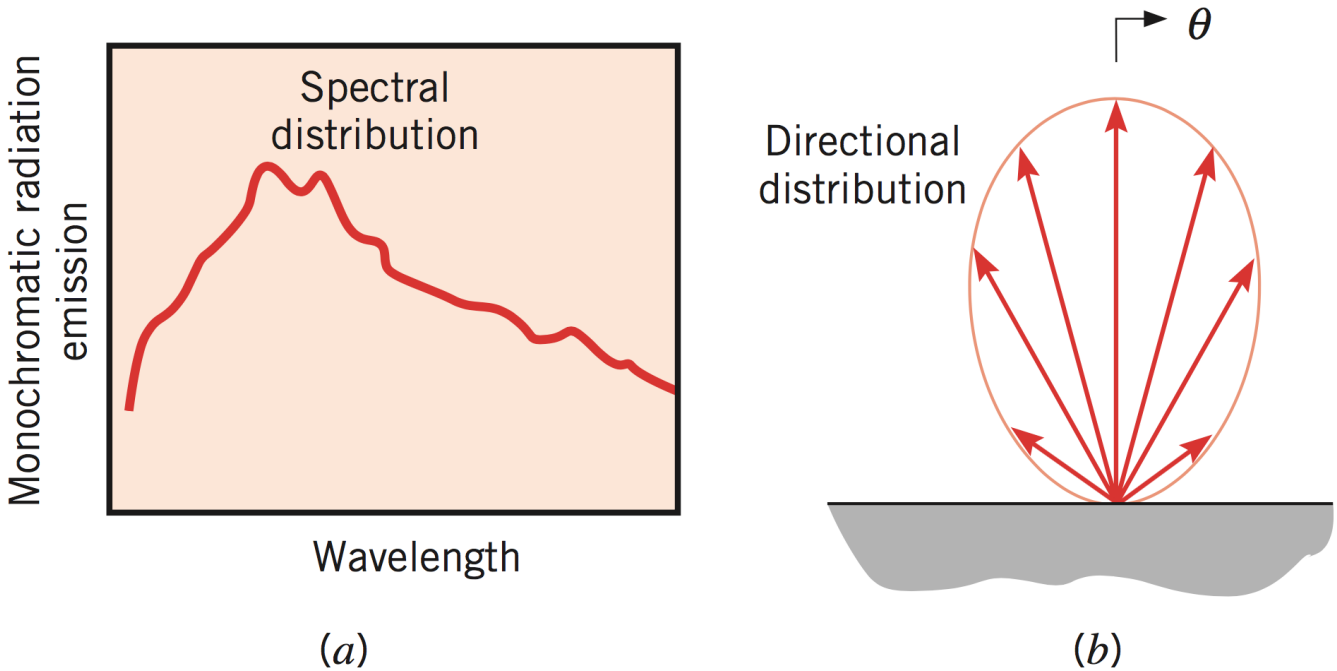

Bergman et al. (2011)

Complexity of radiation: up to **7 independent variables**

- Space: x, y, z
- Time: t
- Direction: θ, ϕ
- Wavelength: λ

EPFL Raman Lidar - Inelastic Scattering

- LIDAR - LIght Detection And Ranging
- Measures water vapor mixing ratio during the day and night
- Raw spatial and time resolutions of 1.25 m and 1 s respectively
- Range 15–500 m
- Solar blind (wavelengths shorter than 0.300 μm, where O_3 absorbs most radiation)
- Raman Scattering (inelastic scattering) - Temp: rotational, MR: rotational/vibrational

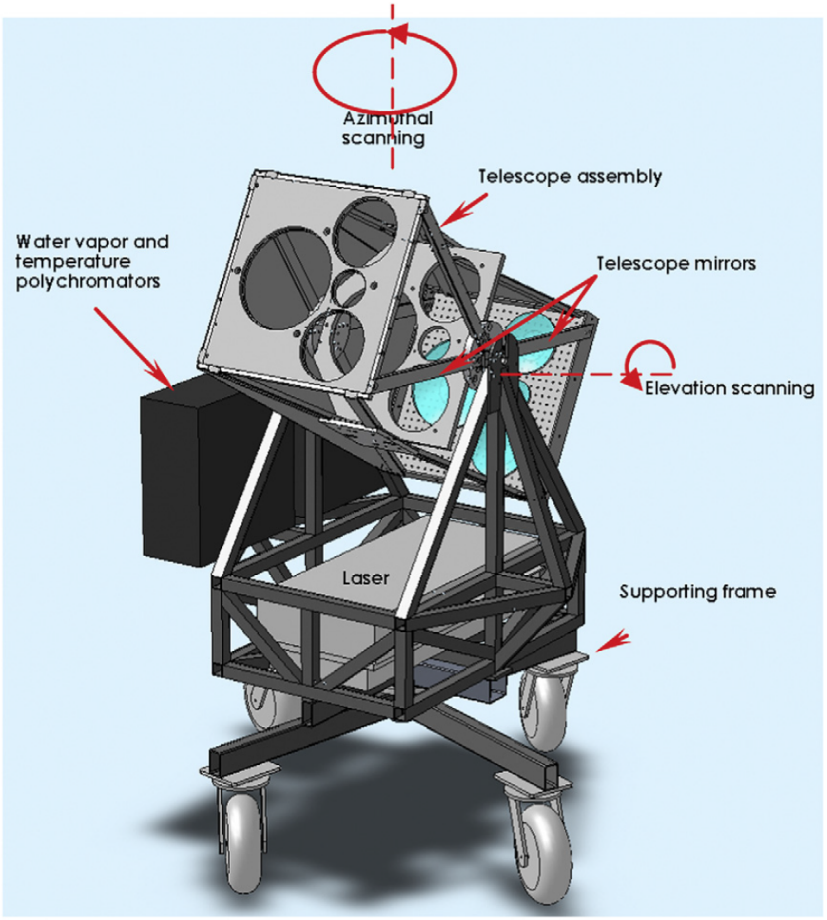

Fig. A.2. 3D projection of the EPFL Raman lidar.

Froidevaux et al. (2013)

Raman Lidar - Seerdorf, CH

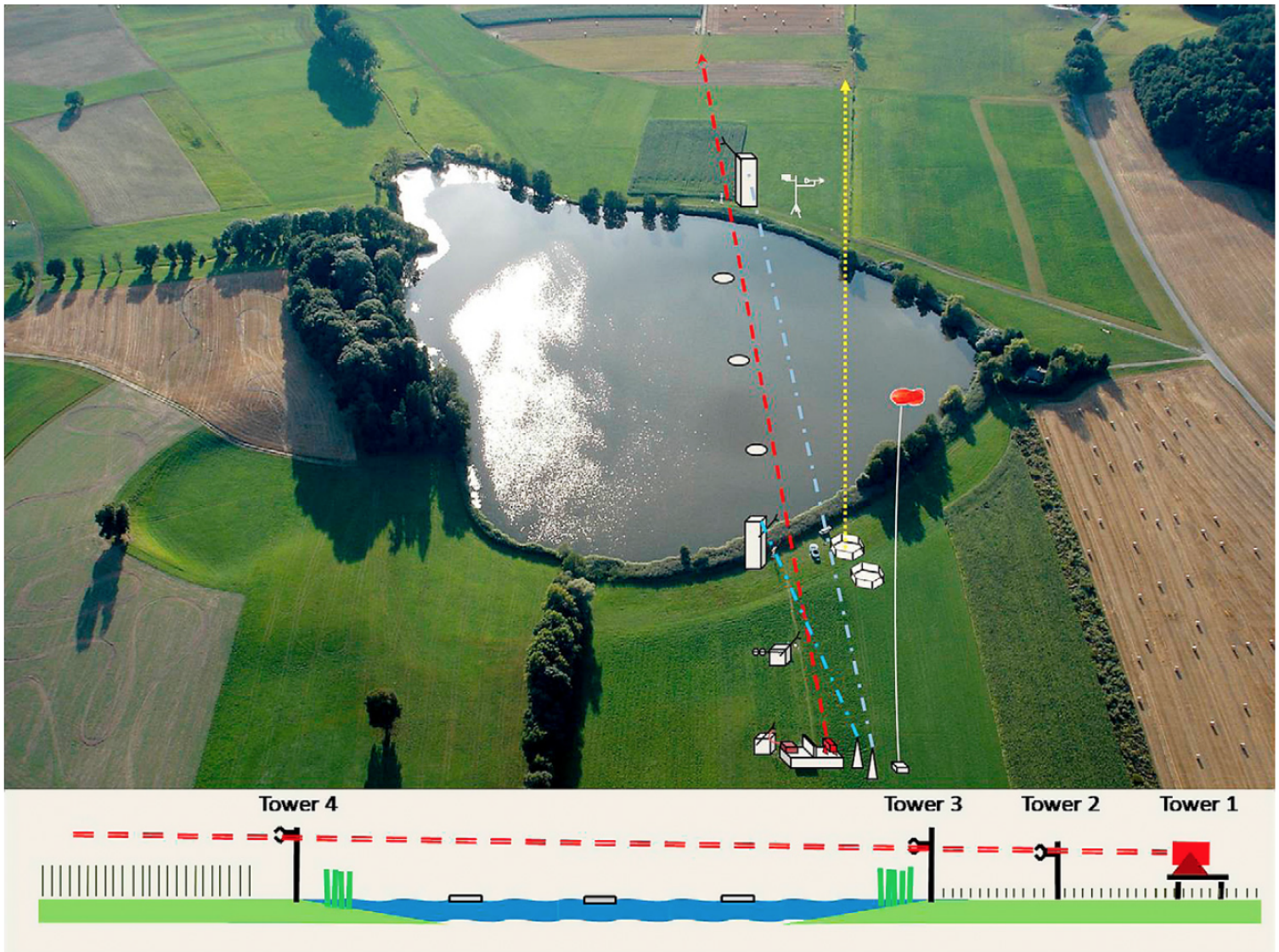

Froidevaux et al. (2013)

Raman Lidar

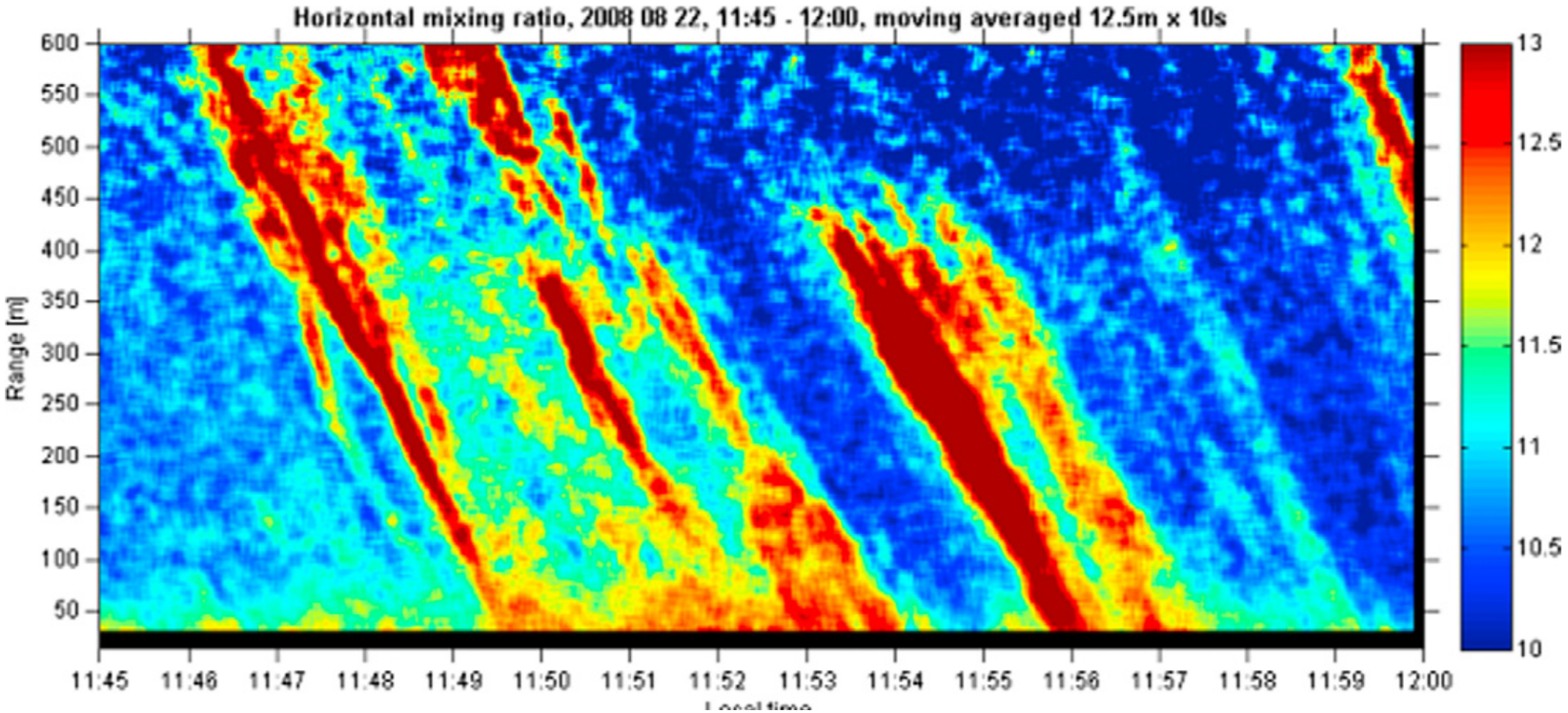

Froidevaux et al. (2013)

Raman Lidar

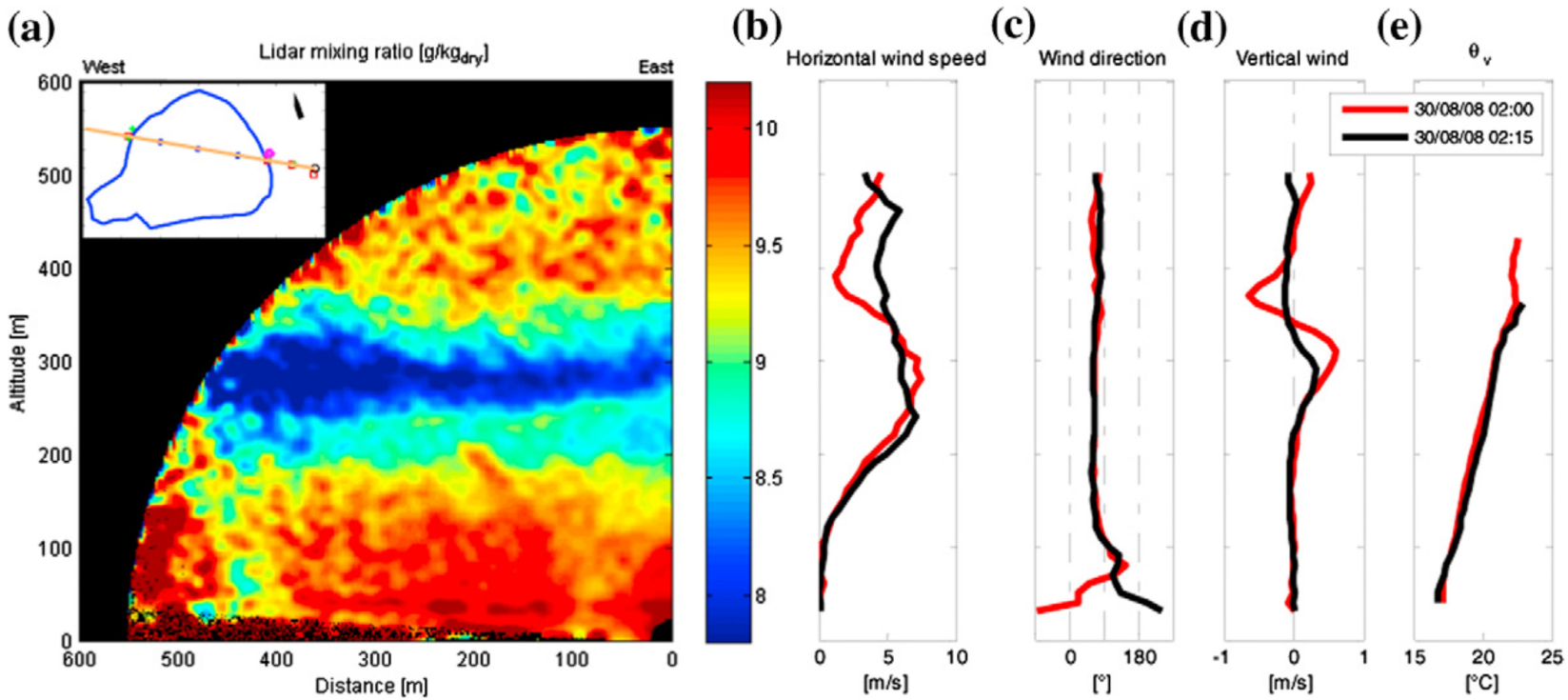

Froidevaux et al. (2013)

Radiation Intensity - Spherical Coordinates and Solid Angle

Directional distribution of thermal radiation is described via solid angles. Solid angles are 2D angular spaces:

- 1D angular pace: $d\alpha = dl/r$
  radians $[\mathrm{rad}]$
  dl: infinitesimal length on a circle

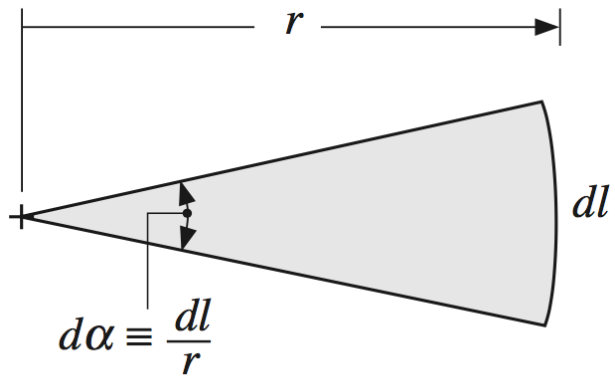

- 2D angular space: $d\omega = dA_n/r^2$
  steradians $[\mathrm{sr}]$
  dA_n: infinitesimal area on a sphere

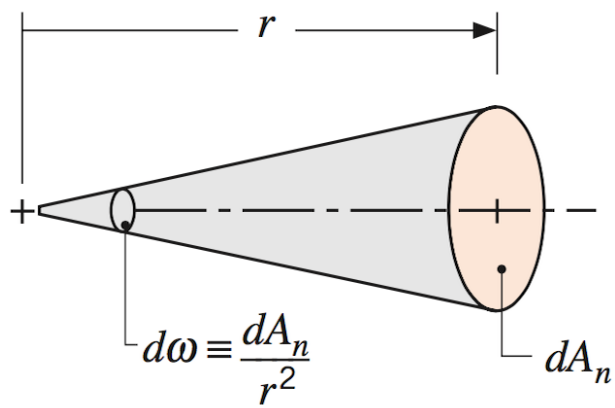

Bergen et al. (2011)

Radiation Intensity - Spherical Coordinates and Solid Angle

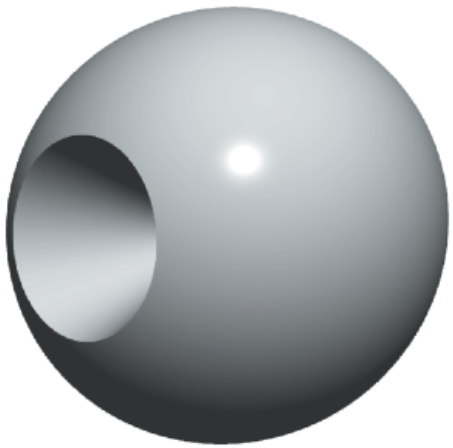

Figure 3.2 — A 1-steradian solid angle removed from a sphere.

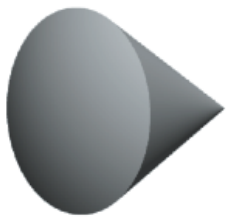

Figure 3.3 — For a solid angle that measures 1 steradian, $A = r^2$.

Adapted by James J. Gross from The Light Measurement Handbook.

Radiation Intensity

Let's consider an emitting point on a surface. This point can radiate into all directions contained within a hemisphere of radius r.

- dA_n: infinitesimal area on the hemisphere of radius r
- θ: polar (zenith) angle
- ϕ: azimuthal angle
- $d\omega$: infinitesimal solid angle

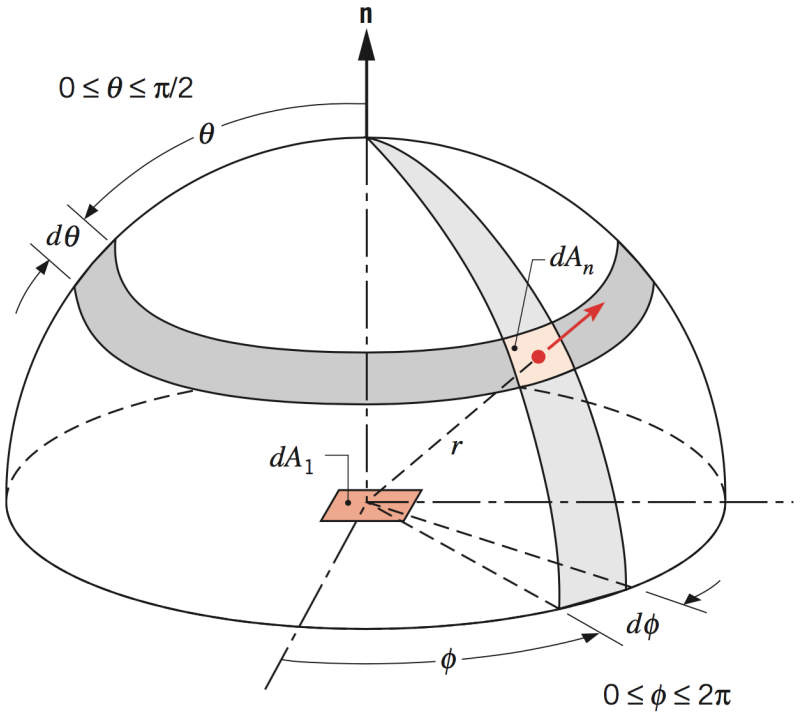

Bergen et al. (2011)

Radiation Intensity - Solid Angle

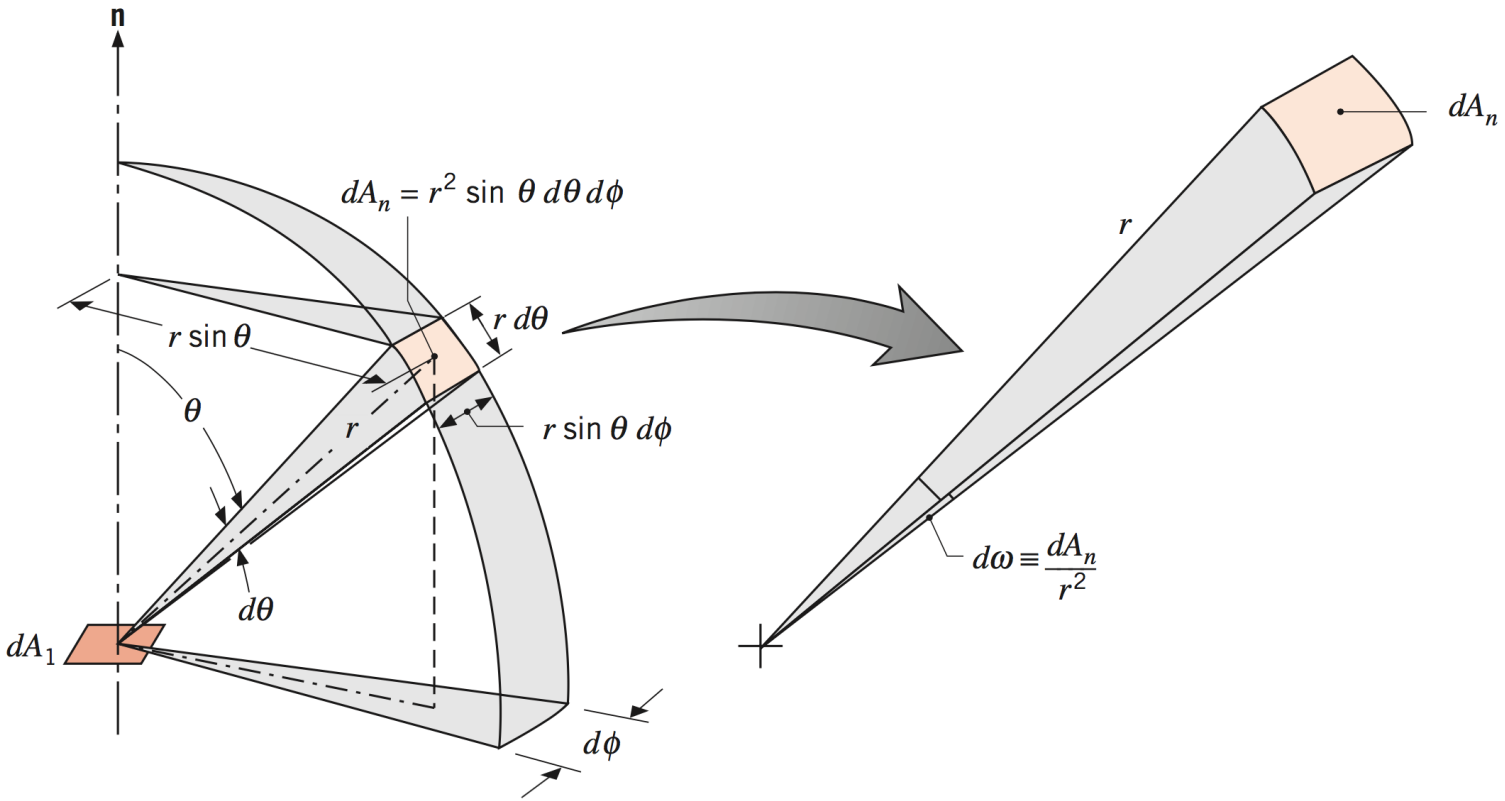

- The infinitesimal area dAn is given by:

$$dA_n = r^2 sin\theta d\theta d\phi$$

- The infinitesimal solid angle is given by:

$$d\omega = dA_n/r^2 = \boxed{sin\theta d\theta d\phi}$$

Spectral Radiance - Lambert's Law

- $L_{(r,s)}$: spectral power per unit area, per unit solid angle, per unit frequency at the point r in the direction of the unit vector s
- **Lambert's Law**: the fractional decrease of spectral radiance is proportional to the mass of the absorbing or scattering material met by the beam along ds

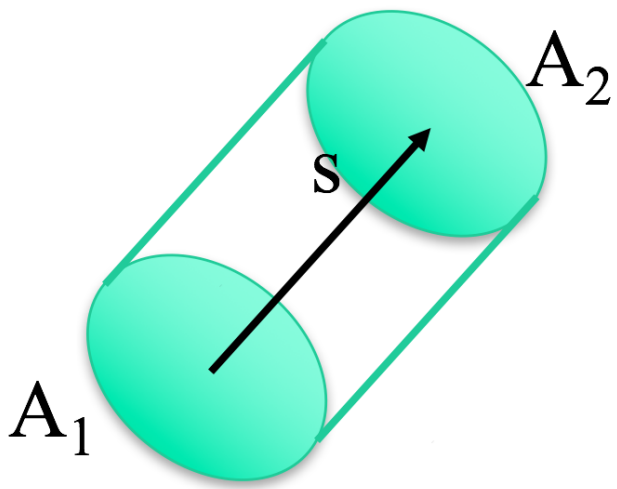

Radiation: Attenuation

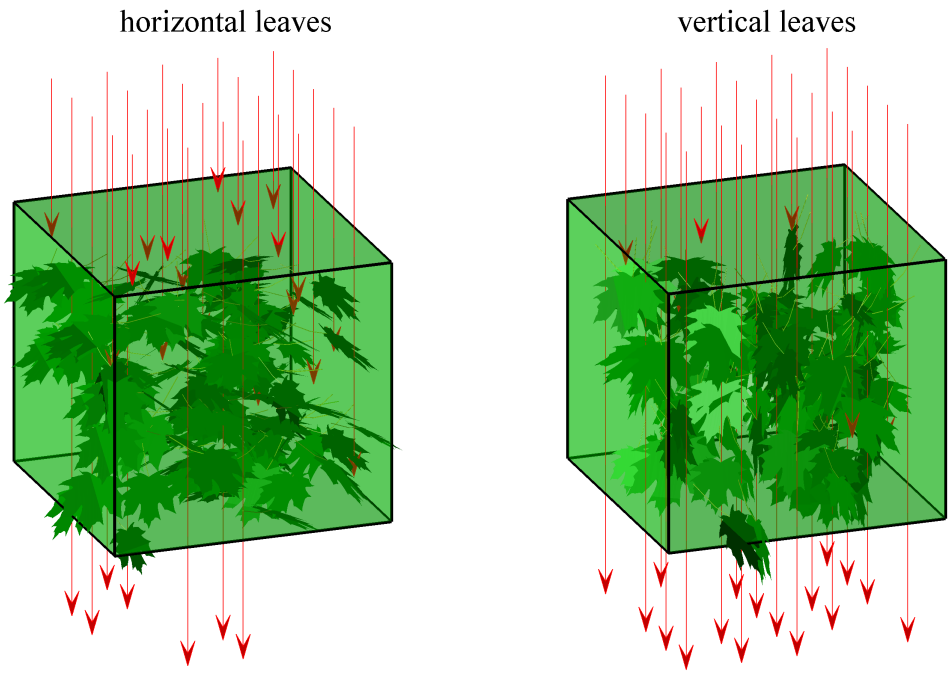

Bailey et al. (2014)

Radiation: Scattering

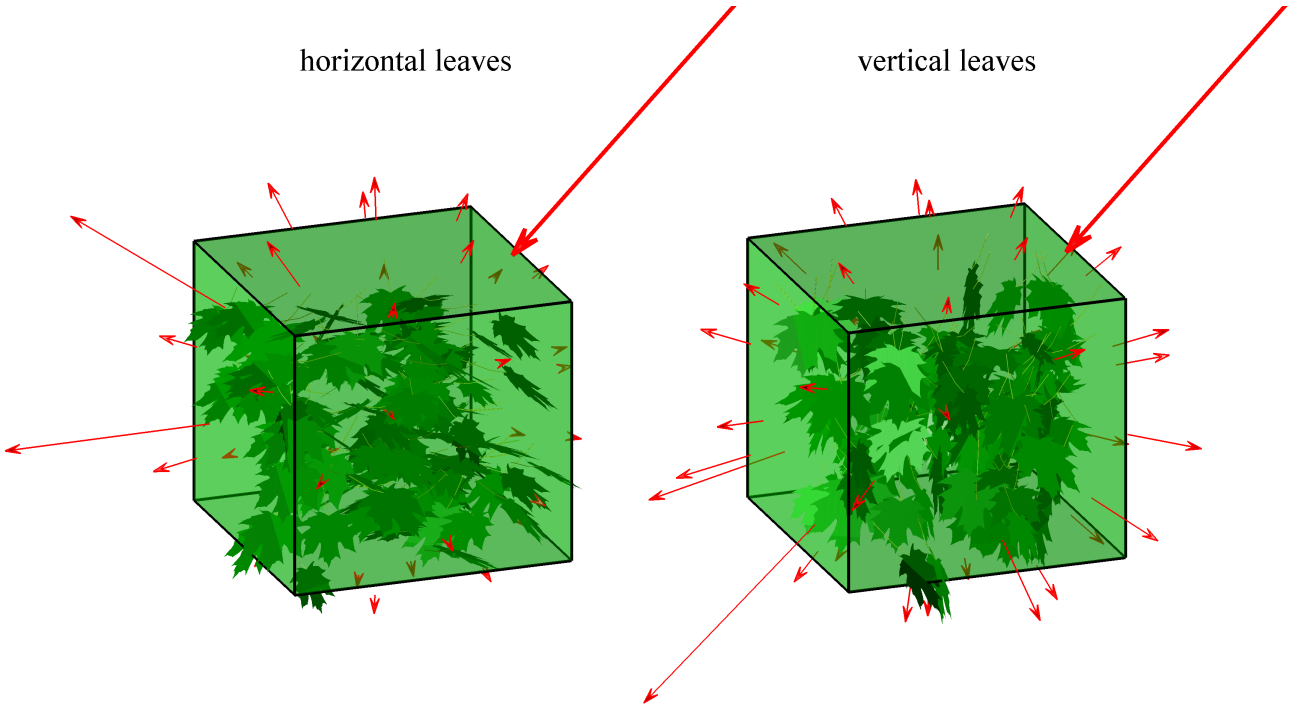

Bailey et al. (2014)

Radiation: Emission

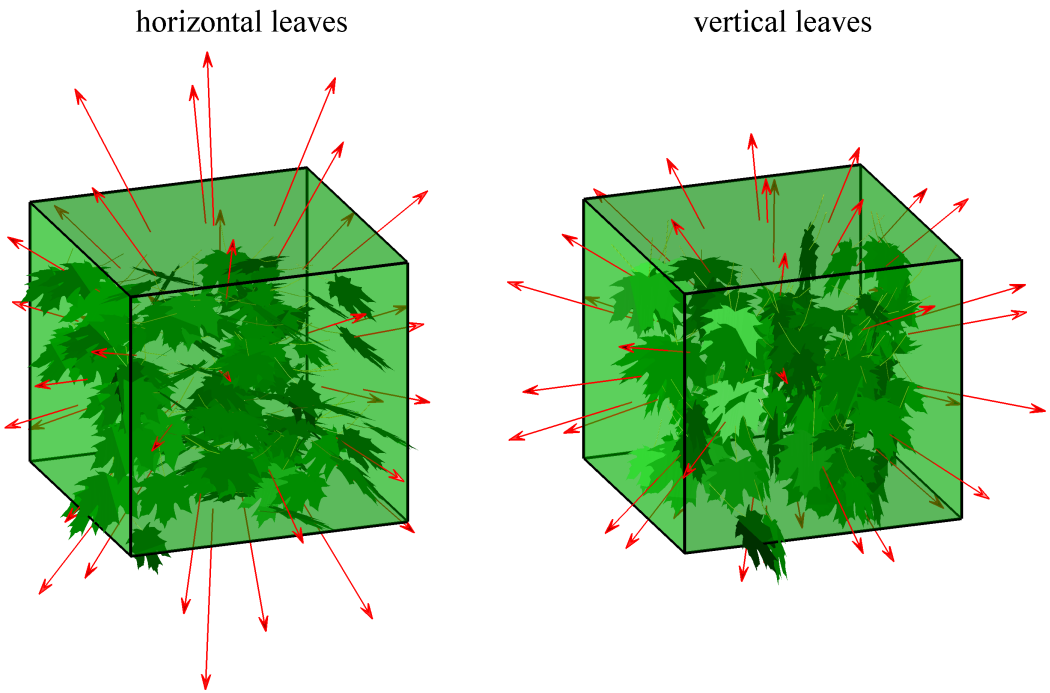

Bailey et al. (2014)

Shortwave and Longwave Radiation

Wien's Displacement Law - wavelength of maximum spectral emissive power

$$\lambda_{\text{max}} = \frac{2898}{T_{\text{abs}}}$$

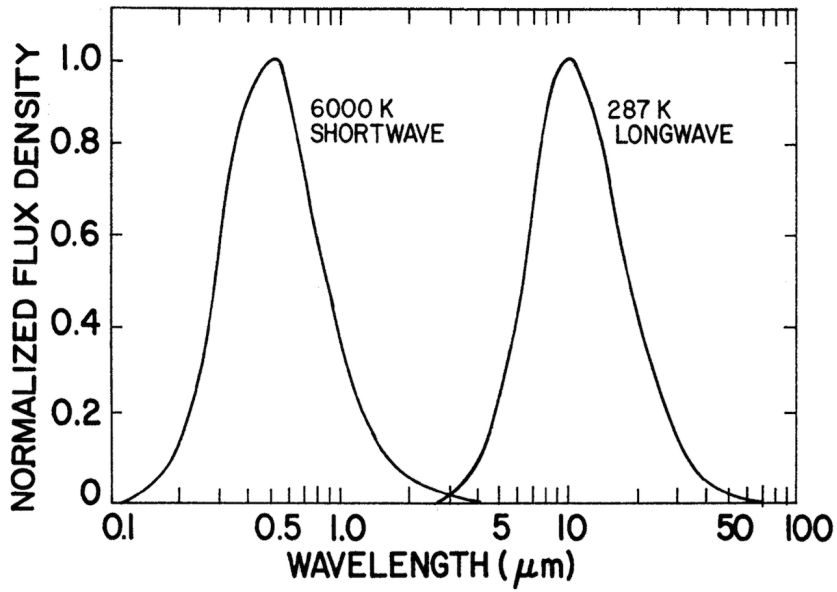

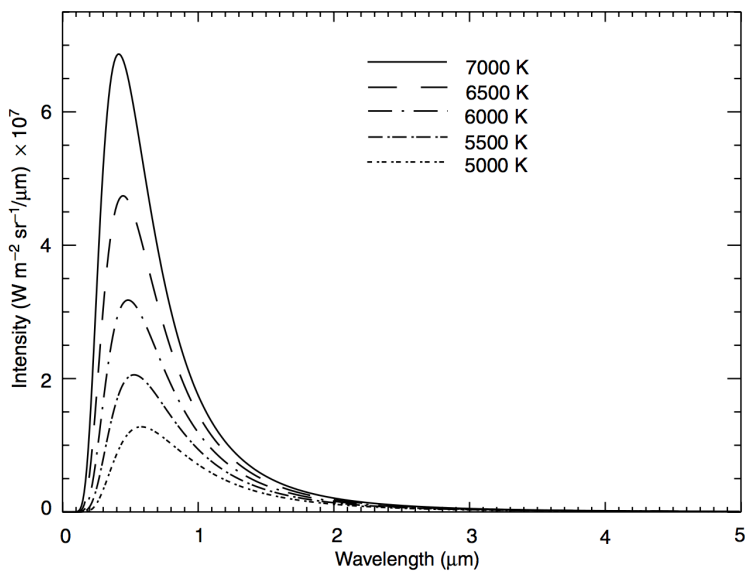

Arya (2001)

Average Global Radiation Balance

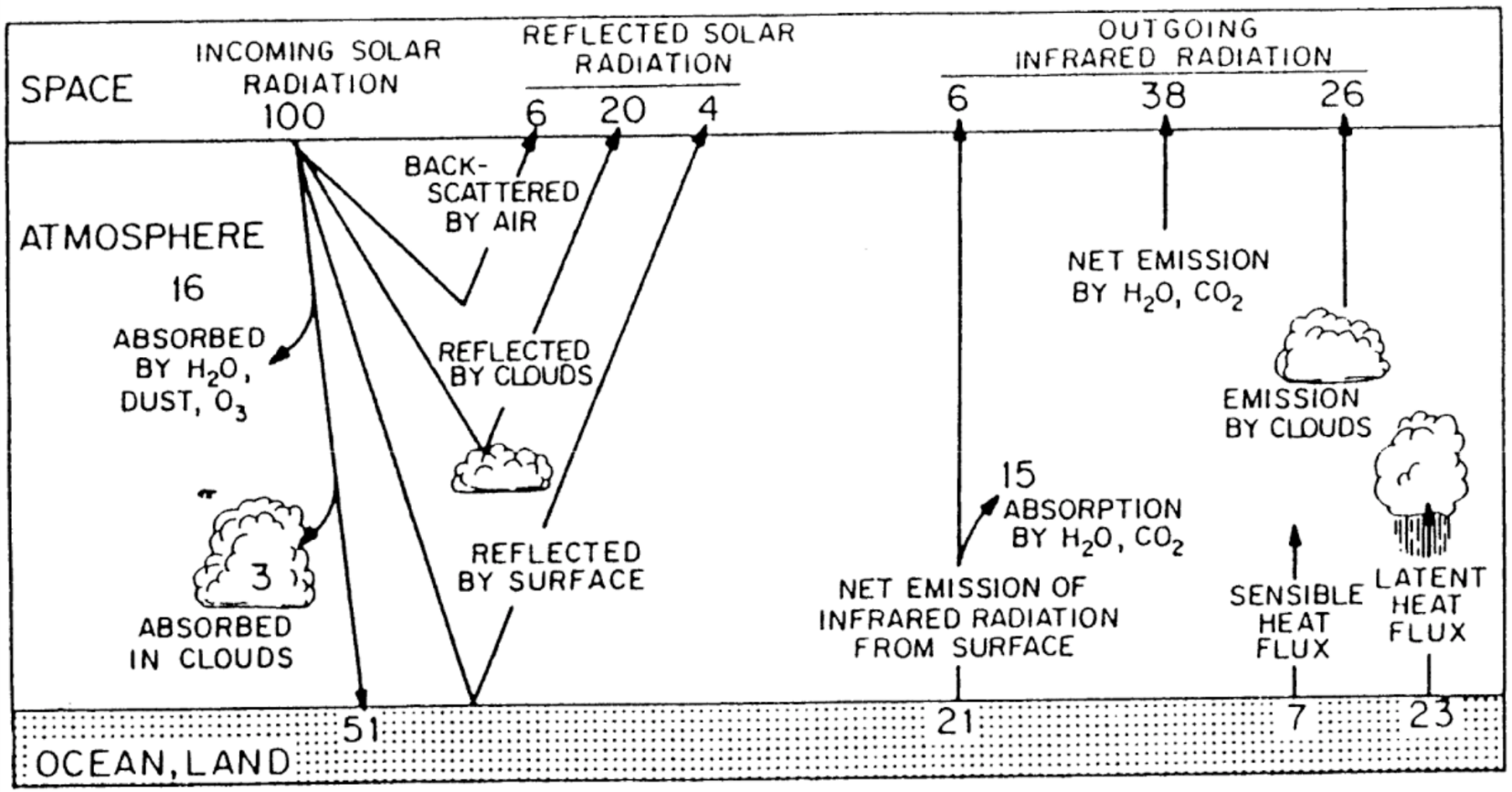

Radiation balance for the atmosphere

Radiative Properties of Surfaces

$$\alpha = \frac{R_S \uparrow}{R_S \downarrow} = \int_{0.15\ \mu m}^{4\ \mu m} \alpha_\lambda d\lambda$$

$$\epsilon = \int_{3\ \mu m}^{100\ \mu m} \epsilon_\lambda d\lambda$$

Albedo of wet grass is a few % less than dry grass

Surface type	Other specifications	Albedo (a)	Emissivity (ε)
Water	Small zenith angle	0.03–0.10	0.92–0.97
	Large zenith angle	0.10–1.00	0.92–0.97
Snow	Old	0.40–0.70	0.82–0.89
	Fresh	0.45–0.95	0.90–0.99
Ice	Sea	0.30–0.45	0.92–0.97
	Glacier	0.20–0.40	
Bare sand	Dry	0.35–0.45	0.84–0.90
	Wet	0.20–0.30	0.91–0.95
Bare soil	Dry clay	0.20–0.40	0.95
	Moist clay	0.10–0.20	0.97
	Wet fallow field	0.05–0.07	
Paved	Concrete	0.17–0.27	0.71–0.88
	Black gravel road	0.05–0.10	0.88–0.95
Grass	Long (1 m)	0.16	0.90
	Short (0.02 m)	0.26	0.95
Agricultural	Wheat, rice, etc.	0.18–0.25	0.90–0.99
	Orchards	0.15–0.20	0.90–0.95
Forests	Deciduous	0.10–0.20	0.97–0.98
	Coniferous	0.05–0.15	0.97–0.99

Compiled from Sellers (1965), Kondratyev (1969), and Oke (1987).

Arya (2001)

Albedo Variability - Murray, Utah

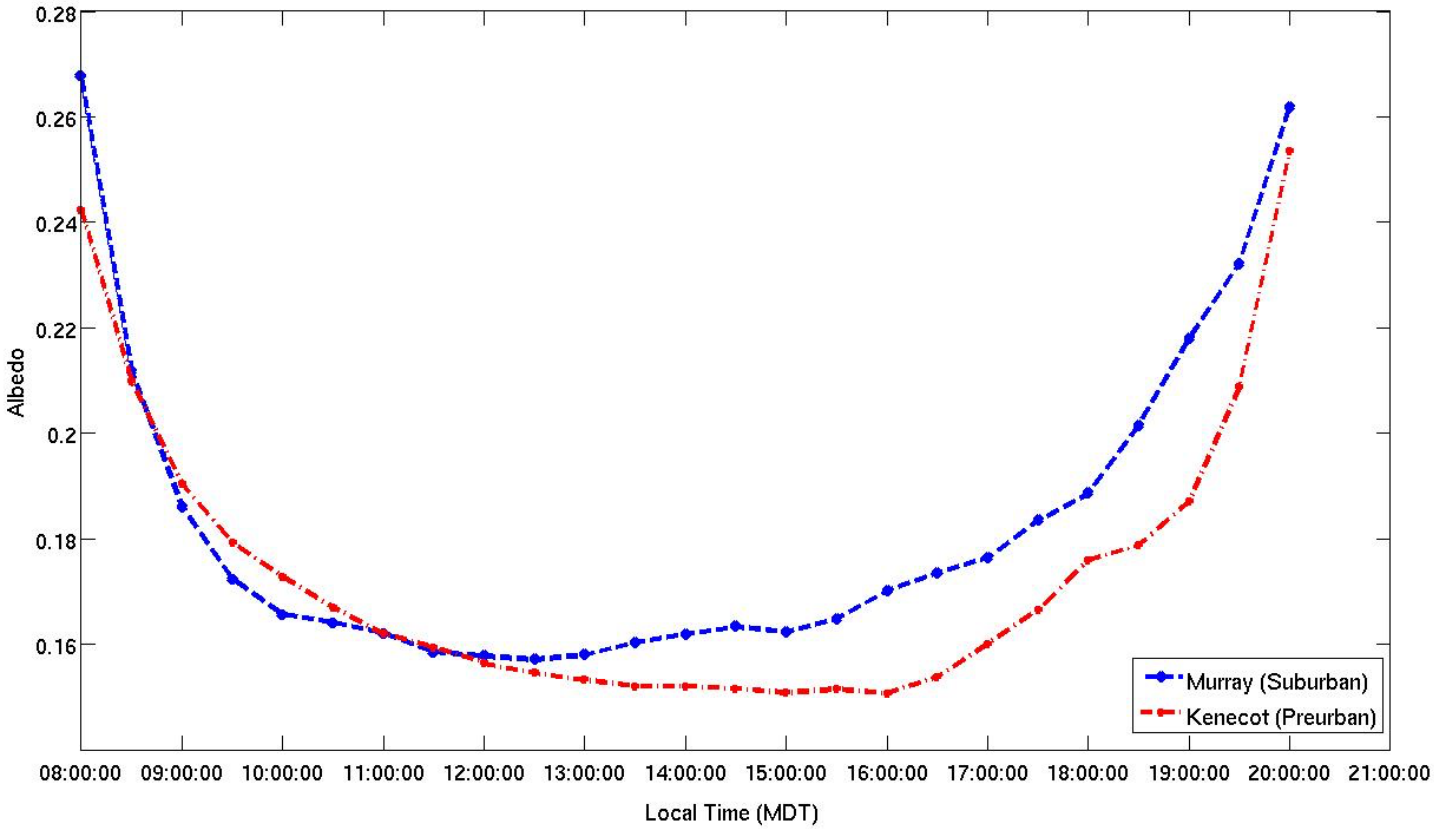

Surface Irradiance

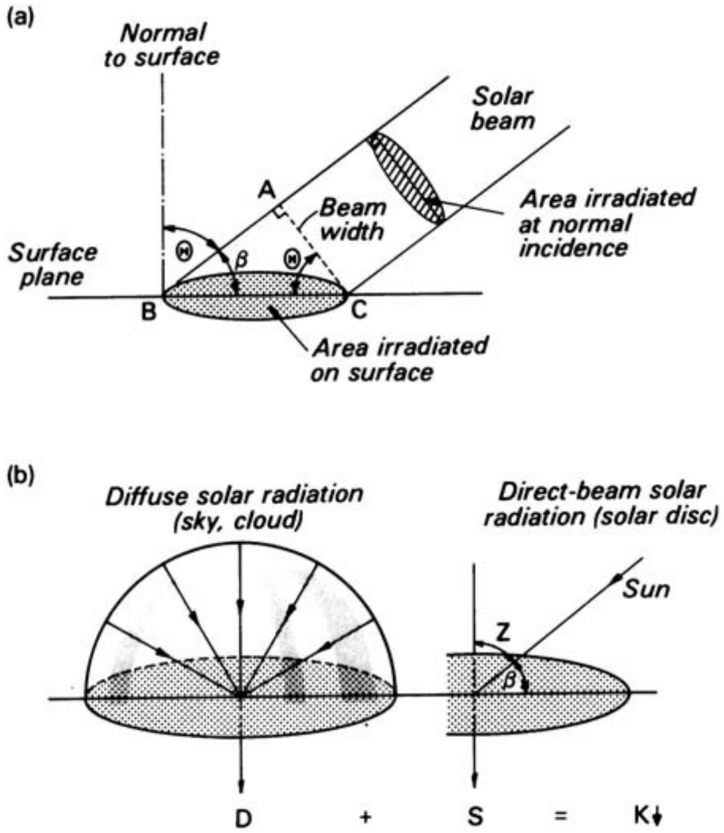

Figure 1.7 (a) Illustration of the areas irradiated by a circular beam on planes placed normal to, and at an angle Θ to, the beam. The radiant energy flux (Js^{-1}) is spread over unit area ($=\pi(0{\cdot}5AC)^2$) at normal incidence but over a larger area ($=\pi(0{\cdot}5BC)^2$) on the surface. The flux density (Wm^{-2}) on the surface (S) is less than that at normal incidence (Si) by the ratio AC/BC=cosΘ or sinß. Therefore, $S=S_i\cos\Theta$ and when $\Theta=0°\cos\Theta=1$ and $S=S_i$. For a horizontal surface Θ=Z the zenith angle of the Sun. (b) The components of incoming solar radiation at the Earth's surface (modified after Monteith, 1973).

- **Direct solar radiation**: portion of short-wave radiation received in a parallel beam "directly" from the sun
- **Diffuse solar radiation**: short-wave radiation reaching the Earth's surface after having been scattered from the direct beam by molecules or other agents in the atmosphere

Surface Irradiance

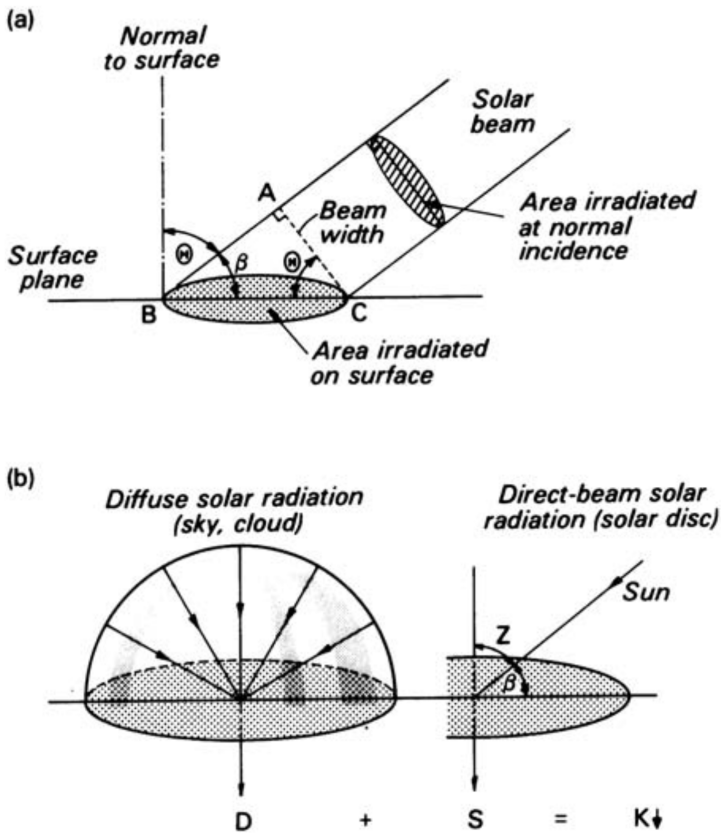

Figure 1.7 (a) Illustration of the areas irradiated by a circular beam on planes placed normal to, and at an angle Θ to, the beam. The radiant energy flux (Js^{-1}) is spread over unit area ($=\pi(0{\cdot}5AC)^2$) at normal incidence but over a larger area ($=\pi(0{\cdot}5BC)^2$) on the surface. The flux density (Wm^{-2}) on the surface (S) is less than that at normal incidence (Si) by the ratio AC/BC=cosΘ or sinß. Therefore, $S=S_i\cos\Theta$ and when $\Theta=0°\cos\Theta=1$ and $S=S_i$. For a horizontal surface Θ=Z the zenith angle of the Sun. (b) The components of incoming solar radiation at the Earth's surface (modified after Monteith, 1973).

- Global = direct solar radiation + diffuse solar radiation
- For clear conditions:
  - diffuse: $\sim 10-20\%$
  - direct: $\sim 80-90\%$

Direct/Diffuse Surface Irradiation

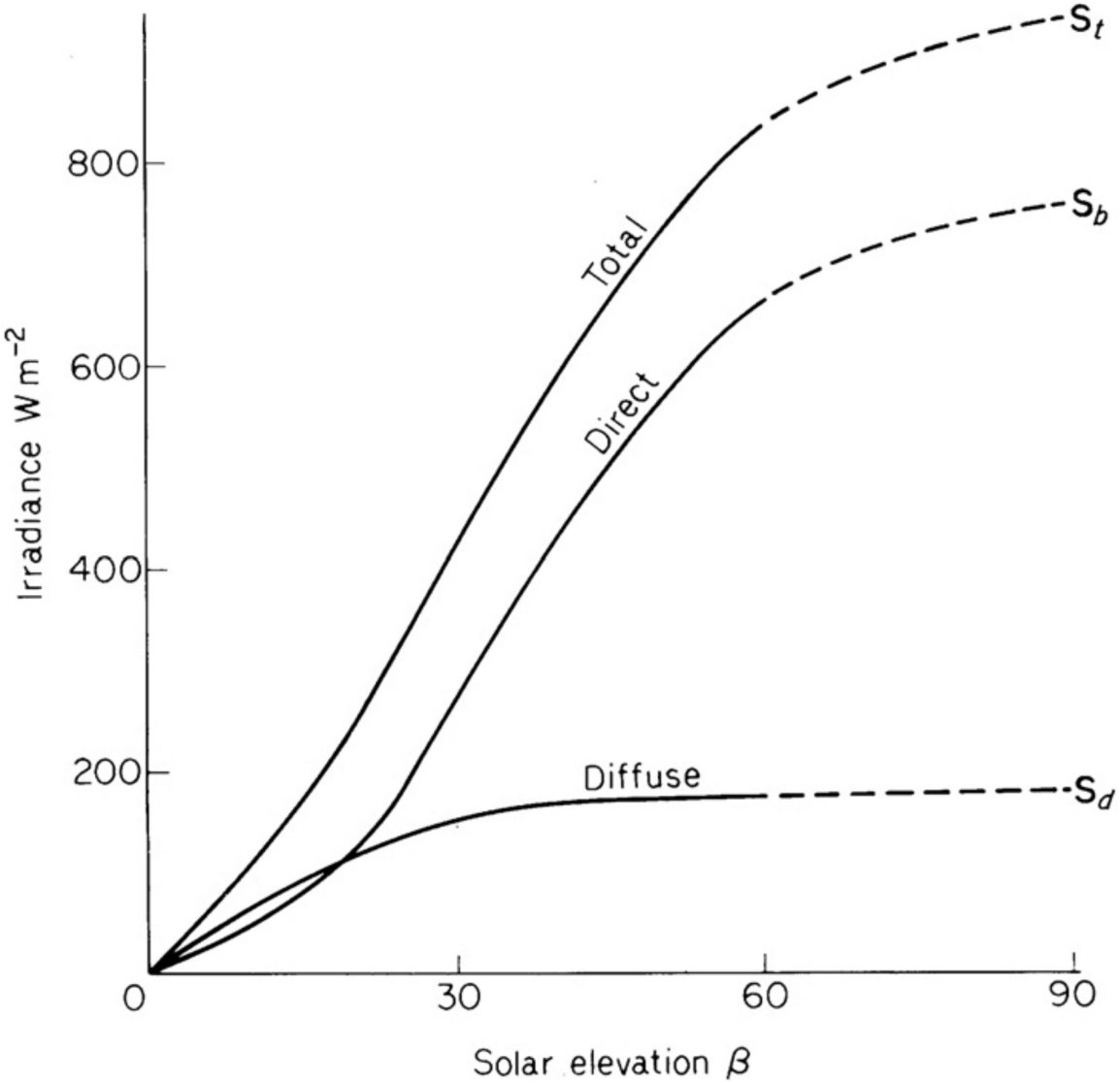

Monteith and Unsworth (2013): Cloudless day, Sutton Bonington, England

Solar "Contant"

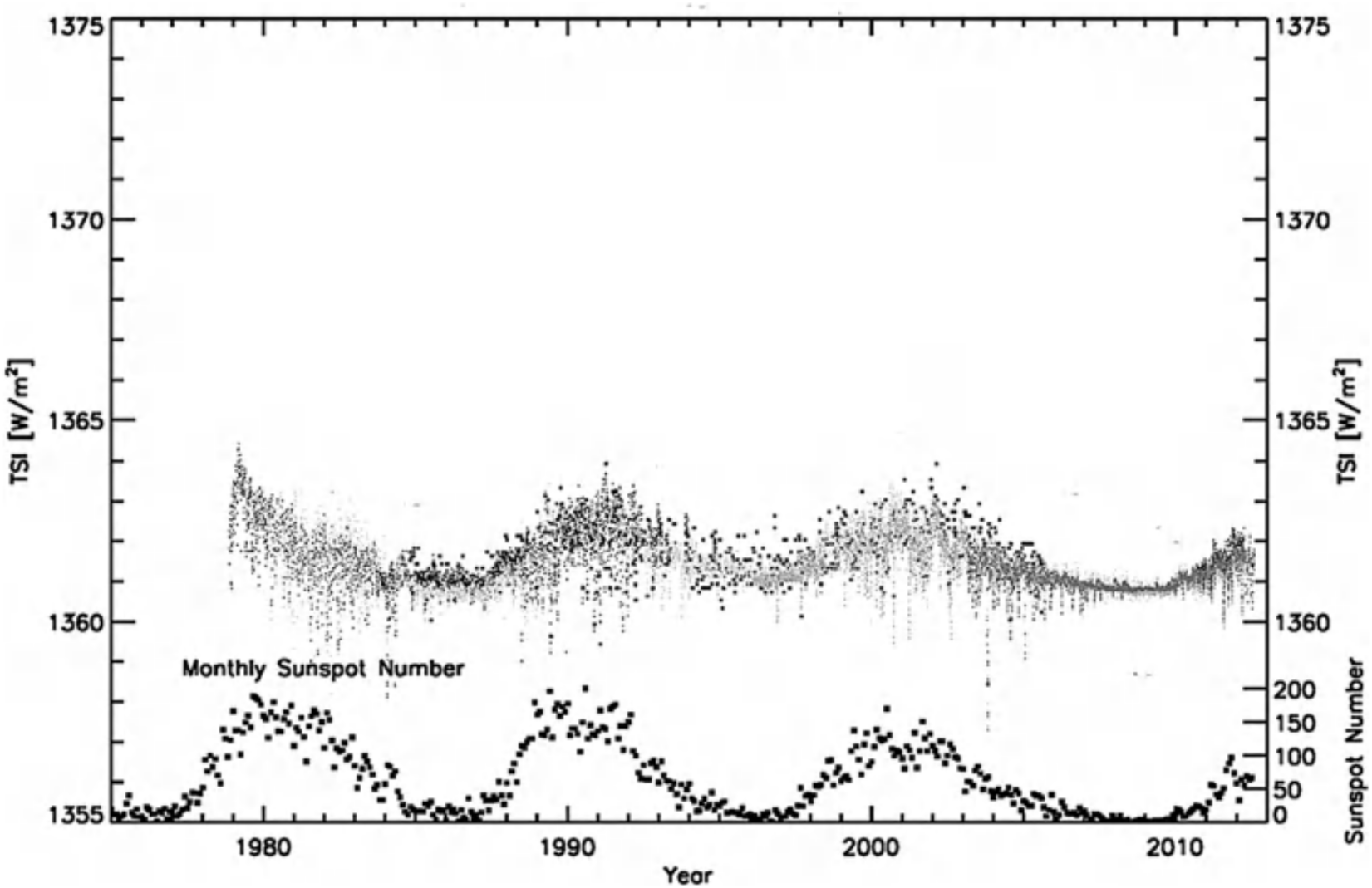

Monteith and Unsworth (2013)

Clear Atmospheric Flux Density of Solar Radiation

Irradiance Spectrum

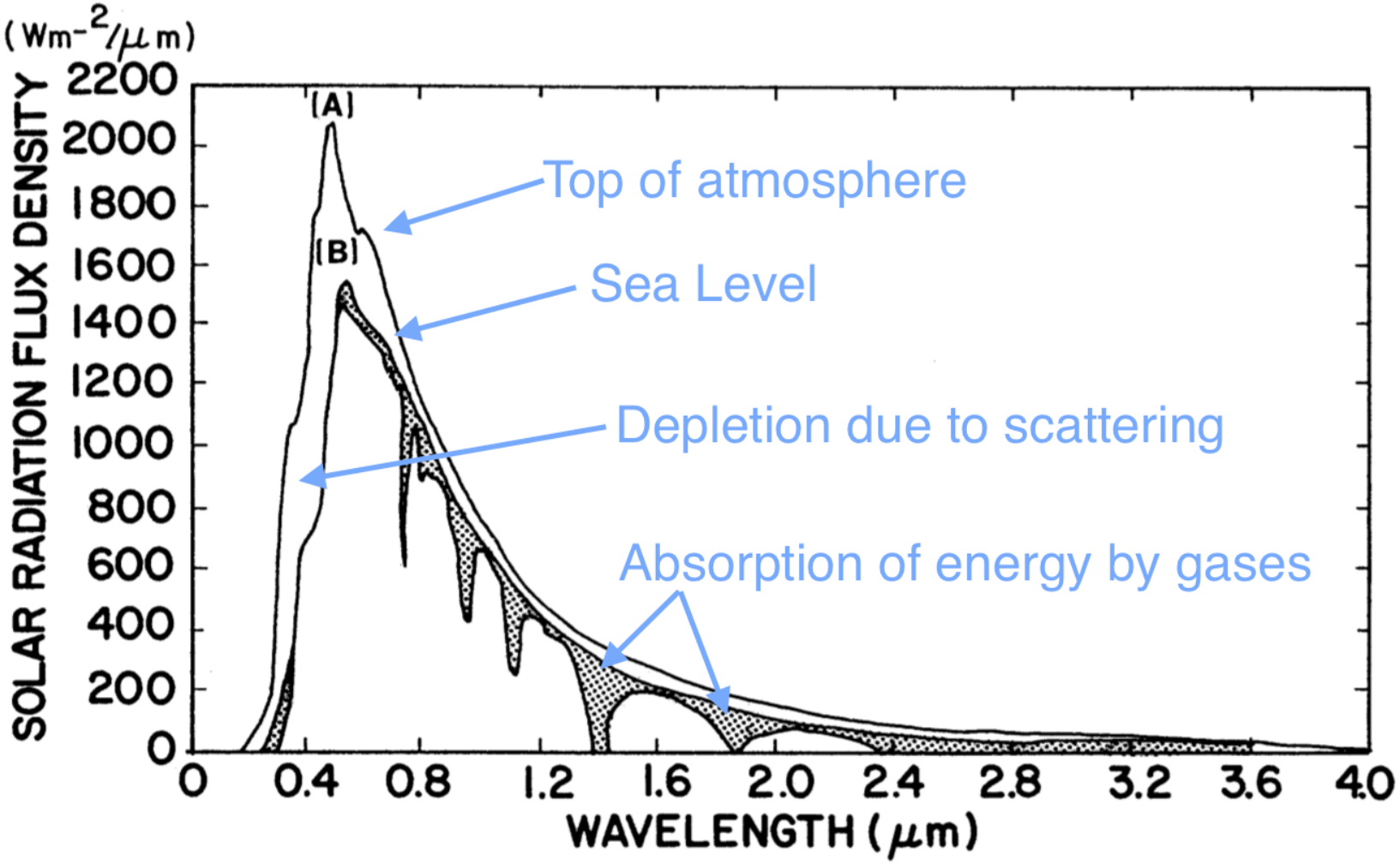

Arya (2001)

Cloudless Absorption Spectra

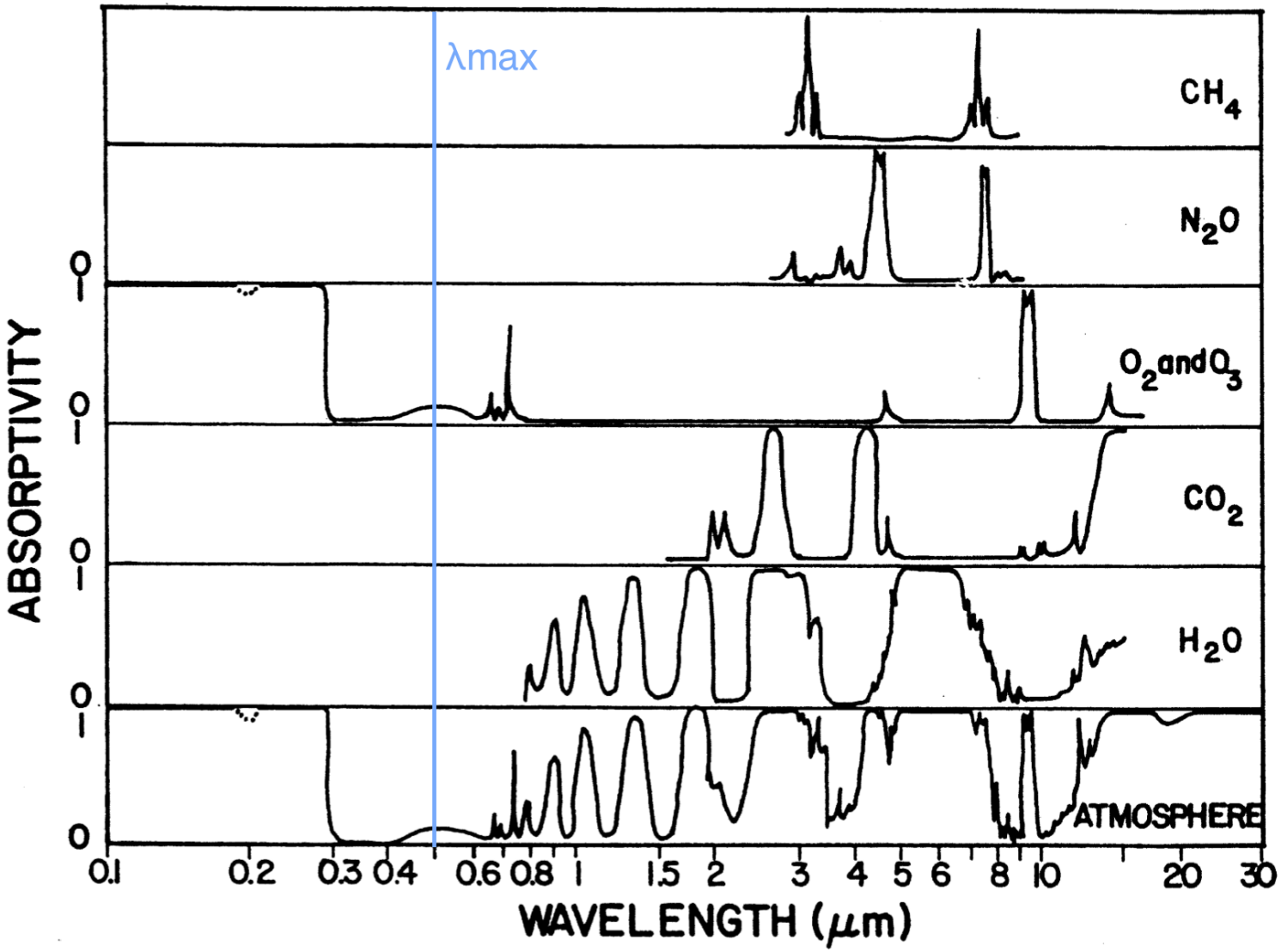

Arya (2001)

Radiation Balance (Clear Diffuse Component)

K – Shortwave; L – Longwave; R_n – Net Radiation

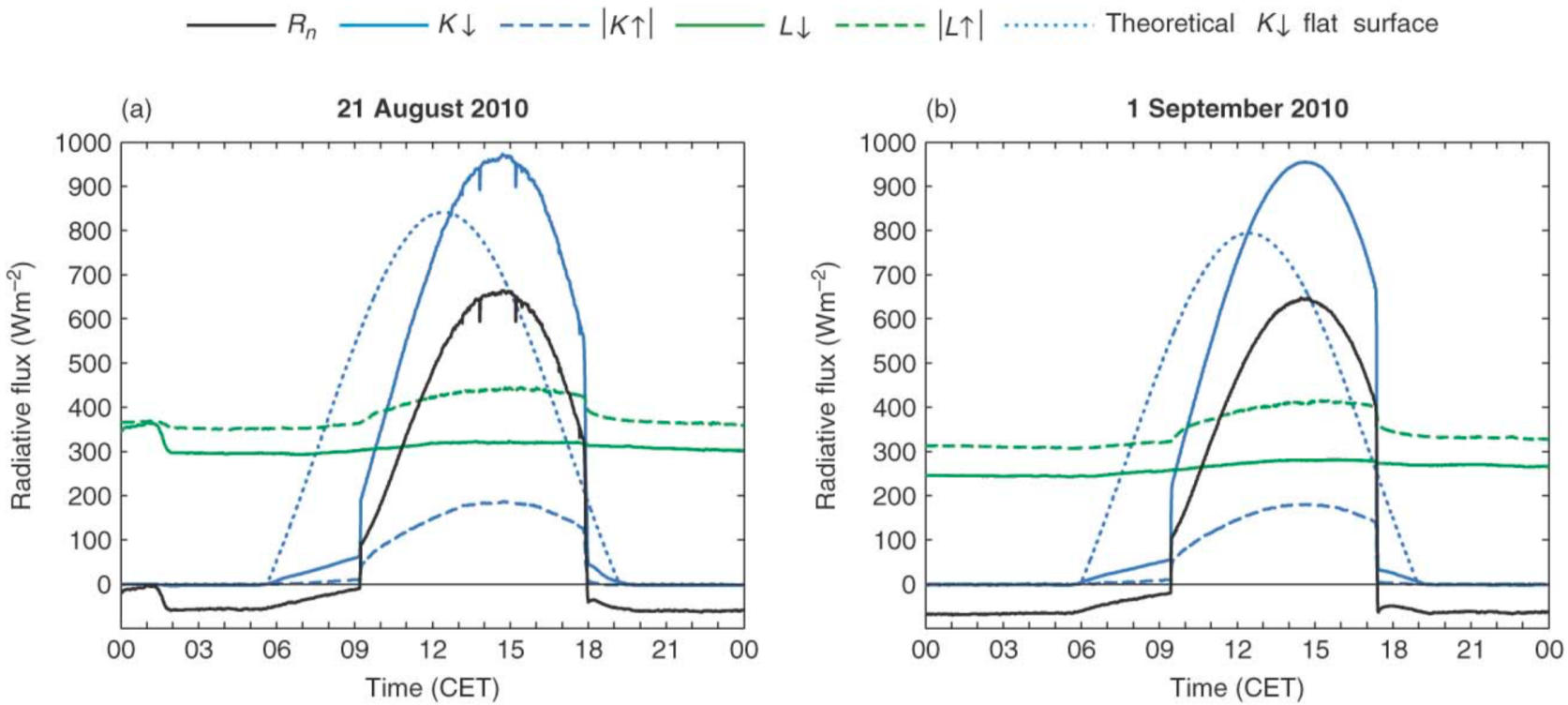

Nadeau et al. (2012)

Radiation Balance

K – Shortwave; L – Longwave

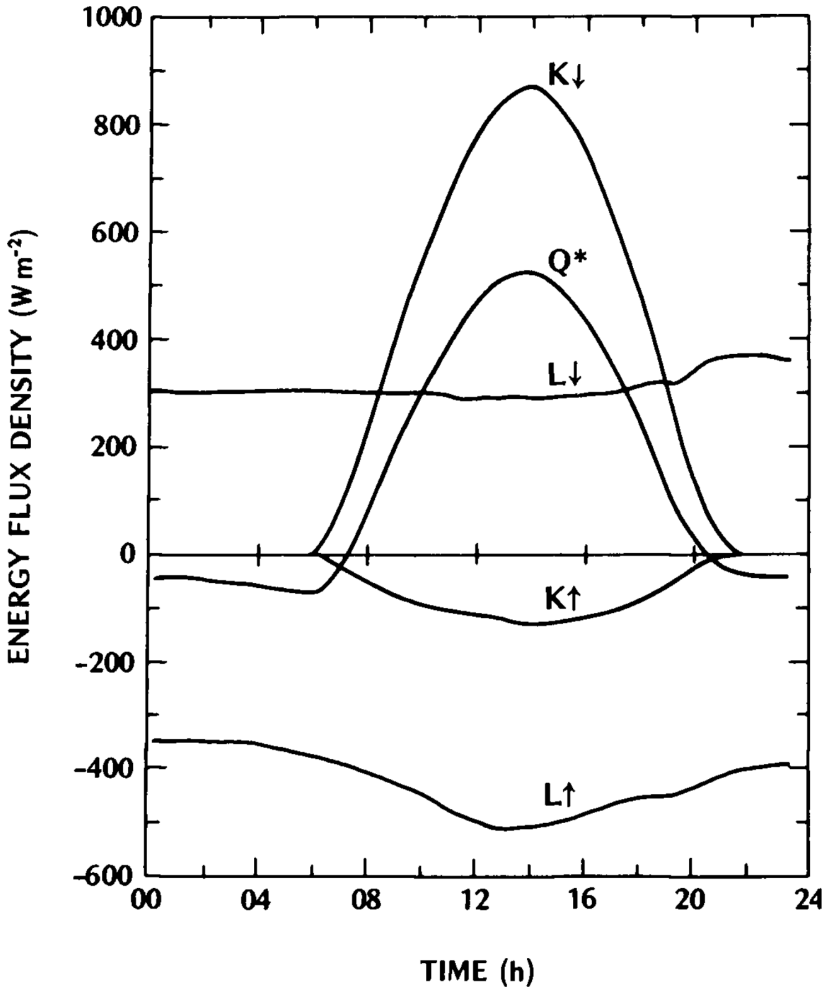

Figure 1.9 Radiation budget components for 30 July 1971, at Matador, Saskatchewan (50°N) over a 0·2 m stand of native grass. Cloudless skies in the morning, increasing cloud in the later afternoon and evening (after Ripley and Redmann, 1976). (*Note*—In the text no signs have been given to individual radiation fluxes, only to net fluxes (K^*, L^* and Q^*). However, in figures such as this radiative inputs to the surface ($K\downarrow$, $L\downarrow$) have been plotted as positive, and outputs ($K\uparrow$, $L\uparrow$) as negative to aid interpretation.) The following table gives the radiation totals for the day (MJ m^{-2}day^{-1}).

$K\downarrow$	27·3	$L\downarrow$	27·5
$K\uparrow$	4·5	$L\uparrow$	36·8
K^*	22·7	L^*	−9·3
$\alpha^\dagger$	0·16	Q^*	13·4

† Dimensionless

Oke (1987)

Slope Solar Beam Irradiance

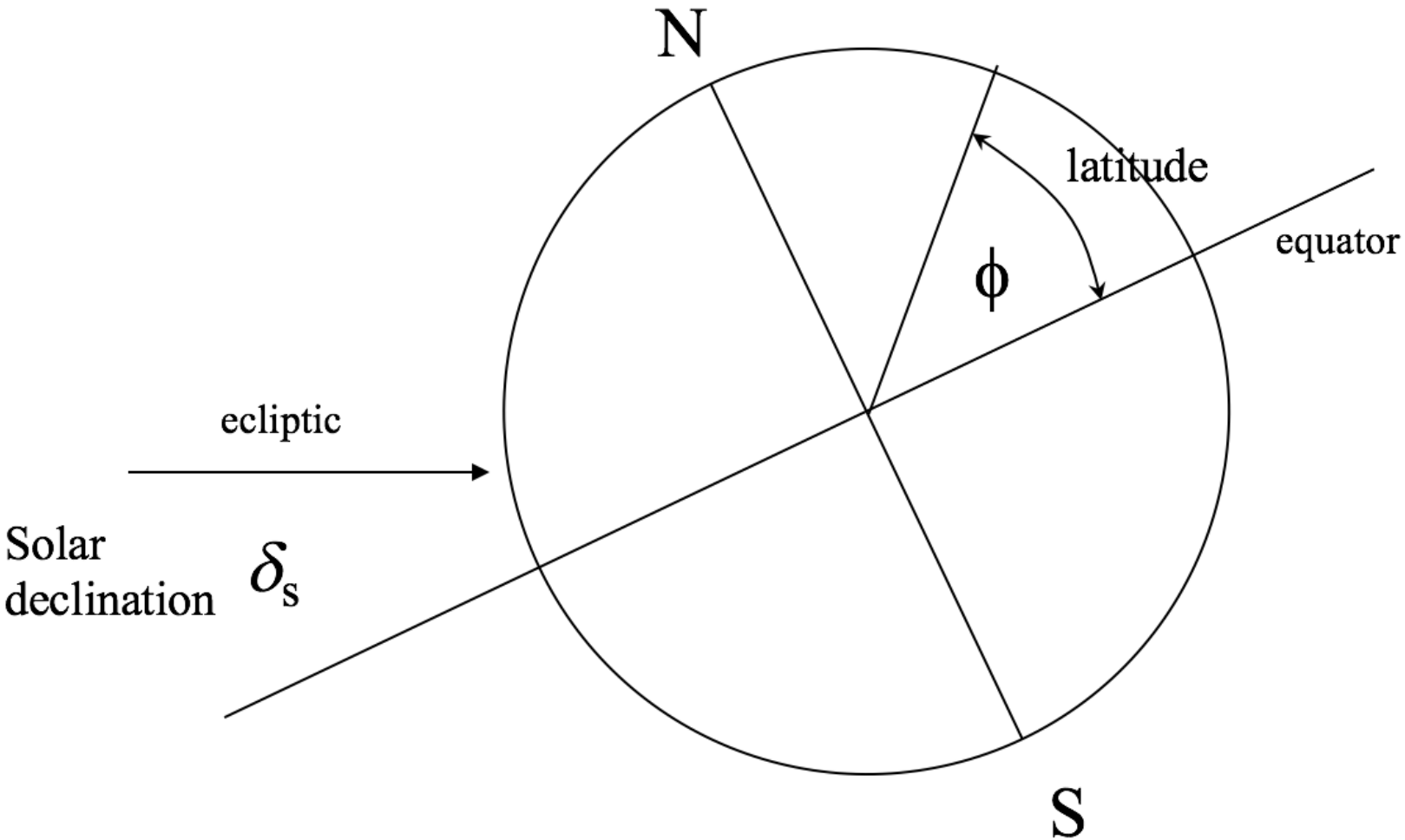

Slope Solar Beam Irradiance

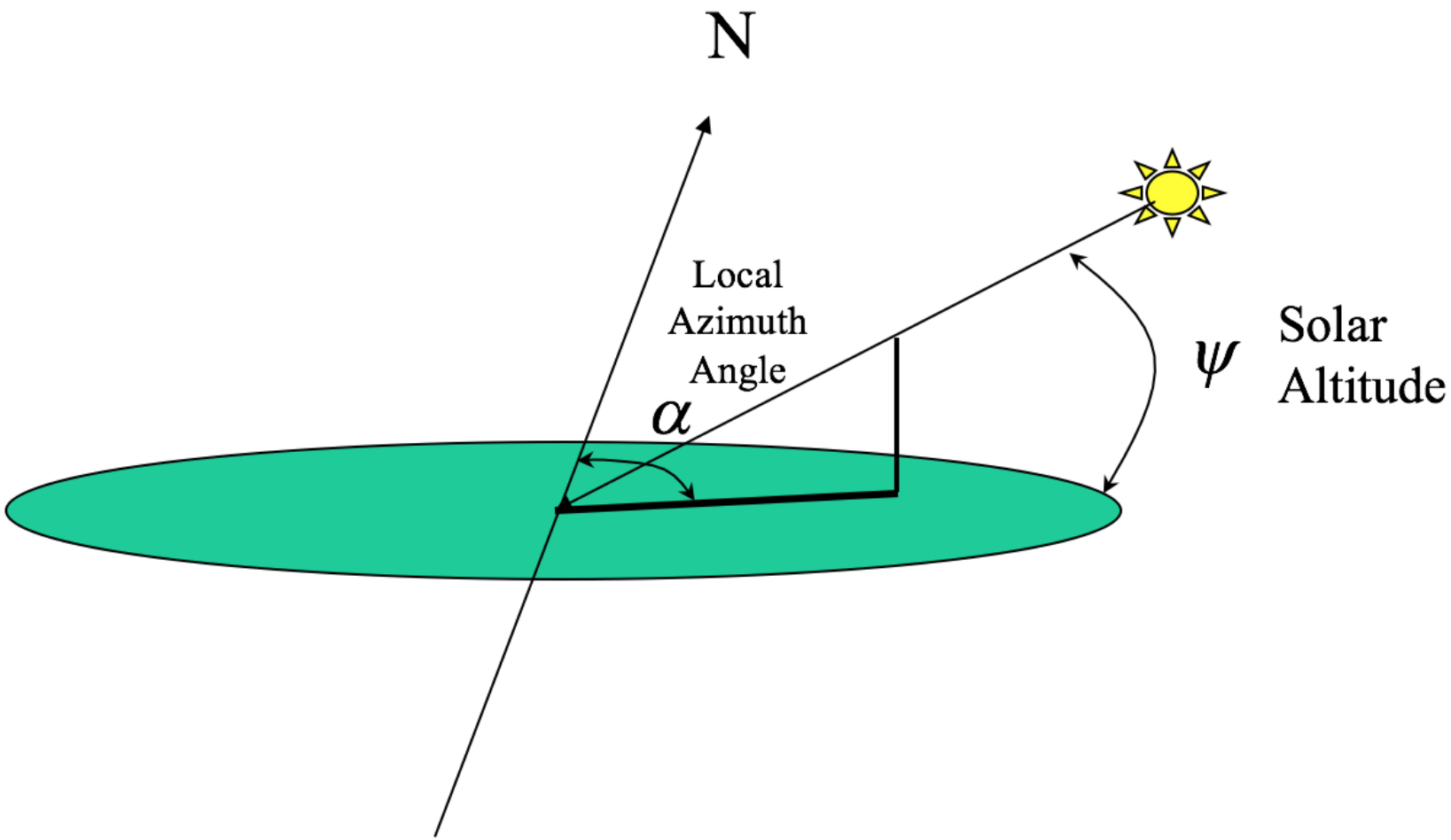

Slope Solar Beam Irradiance

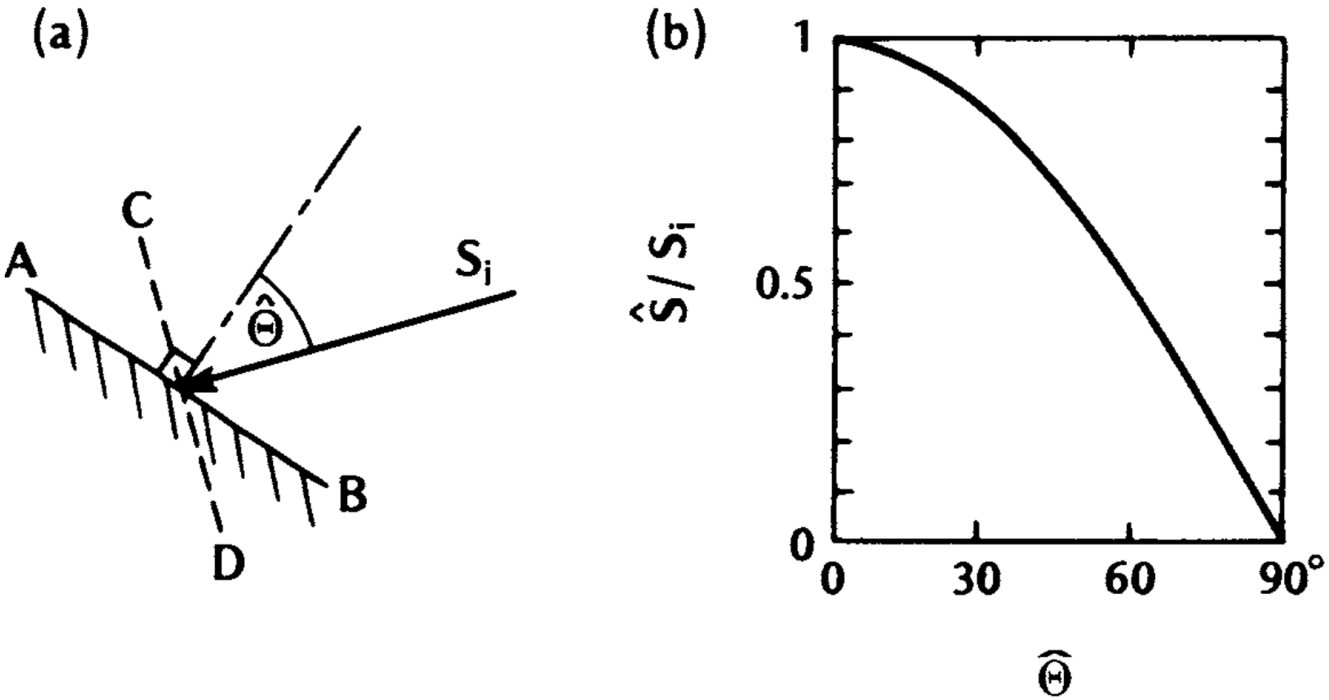

Figure 5.7 (a) Diagrammatic representation of the angle $\hat{\Theta}$ between the surface and the incident direct-beam short-wave radiation, $\hat{S}$. (b) The form of the cosine law of illumination.

Oke (1987)

$$\hat{S} = S_i cos\hat{\Theta}$$

Slope Solar Beam Irradiance

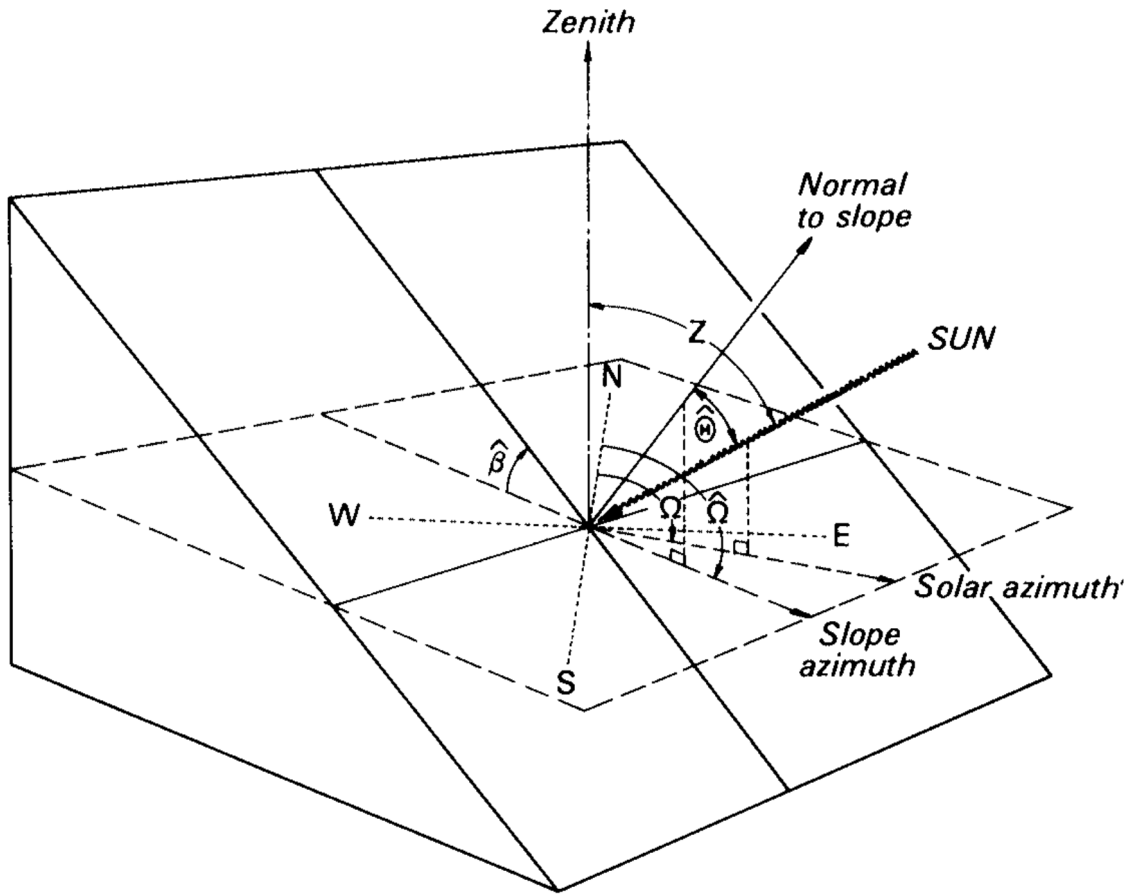

Z – *Zenith angle*
$\hat{\beta}$ – *Slope angle*
Ω – *Solar azimuth angle*
$\hat{\Omega}$ – *Slope azimuth angle*
$\hat{\theta}$ – *Angle of incidence (between Sun and the*

Oke (1987)

Direct Beam Solar Radiation on Sloped Surfaces

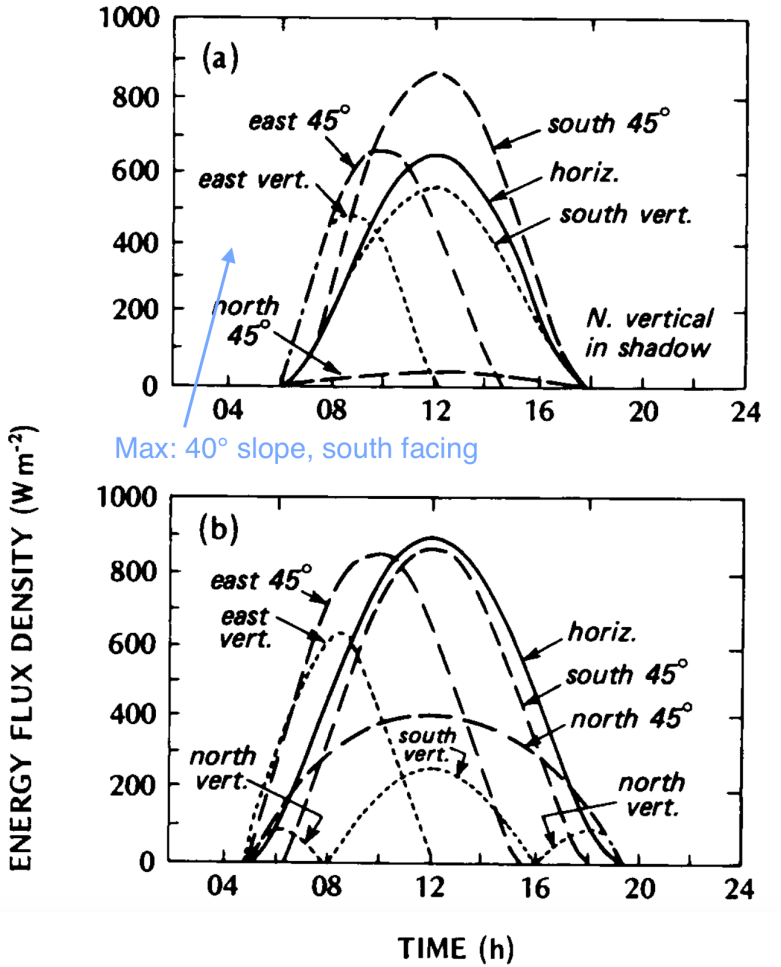

Figure 5.8 The diurnal variation of direct-beam solar radiation upon surfaces with different angles of slope and aspect at latitude 40°N for (a) the equinoxes (21 March, 21 September), (b) summer solstice (22 June), and (c) winter solstice (22 December) (after Gates, 1965).

Oke (1987)

Direct Beam Solar Radiation on Sloped Surfaces

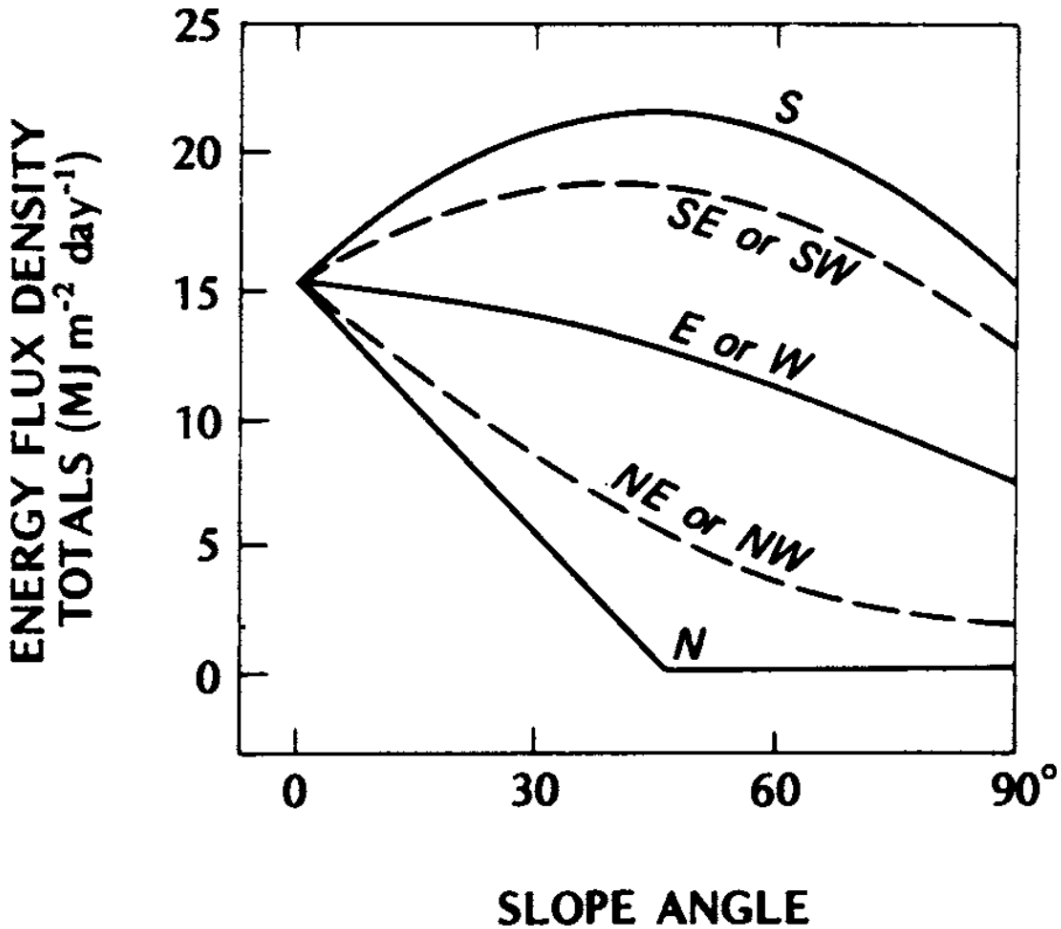

Figure 5.9 Total daily direct-beam solar radiation ($\hat{S}$) incident upon slopes of differing angle and aspect at latitude 45°N at the times of the equinoxes (diagram constructed by Monteith, 1973, using data from Garnier and Ohmura, 1968).

Oke (1987)